Blockade of IL-6R prevents preterm birth and adverse neonatal outcomes

Marcelo Farias-Jofre,[a,b,c,n] Roberto Romero,[a,d,e,n,**] Jose Galaz,[a,b,c,n] Yi Xu,[a,b] Derek Miller,[a,b,f] Valeria Garcia-Flores,[a,b,f] Marcia Arenas-Hernandez,[a,b] Andrew D. Winters,[a,g] Bruce A. Berkowitz,[h] Robert H. Podolsky,[i] Yimin Shen,[j] Tomi Kanninen,[a,b] Bogdan Panaitescu,[a,b] Catherine R. Glazier,[k] Roger Pique-Regi,[a,b,l] Kevin R. Theis,[a,b,g] and Nardhy Gomez-Lopez[a,b,f,g,l,m,*]

[a]Pregnancy Research Branch, Division of Obstetrics and Maternal-Fetal Medicine, Division of Intramural Research, *Eunice Kennedy Shriver* National Institute of Child Health and Human Development, National Institutes of Health, U.S. Department of Health and Human Services (NICHD/NIH/DHHS), Bethesda, MD, USA
[b]Department of Obstetrics and Gynecology, Wayne State University School of Medicine, Detroit, MI, USA
[c]Division of Obstetrics and Gynecology, School of Medicine, Faculty of Medicine, Pontificia Universidad Catolica de Chile, Santiago, Chile
[d]Department of Obstetrics and Gynecology, University of Michigan, Ann Arbor, MI, USA
[e]Department of Epidemiology and Biostatistics, Michigan State University, East Lansing, MI, USA
[f]Department of Obstetrics and Gynecology, Washington University School of Medicine, St. Louis, MO, USA
[g]Department of Biochemistry, Microbiology, and Immunology, Wayne State University School of Medicine, Detroit, MO, USA
[h]Department of Ophthalmology, Visual and Anatomical Sciences, Wayne State University School of Medicine; Detroit, MI, USA
[i]Division of Biostatistics and Design Methodology, Center for Translational Research, Children's National Hospital, Silver Spring, MD, USA
[j]Department of Radiology, School of Medicine, Wayne State University School of Medicine, Detroit, MI, USA
[k]UCD School of Medicine, University College Dublin, Belfield, Dublin 4, Ireland
[l]Center for Molecular Medicine and Genetics, Wayne State University School of Medicine, Detroit, MI, USA
[m]Department of Pathology and Immunology, Washington University School of Medicine, St. Louis, MO, USA

eBioMedicine
2023;98: 104865
Published Online xxx
https://doi.org/10.1016/j.ebiom.2023.104865

Summary

Background **Preterm birth preceded by spontaneous preterm labour often occurs in the clinical setting of sterile intra-amniotic inflammation (SIAI), a condition that currently lacks treatment.**

Methods **Proteomic and scRNA-seq human data were analysed to evaluate the role of IL-6 and IL-1α in SIAI. A C57BL/6 murine model of SIAI-induced preterm birth was developed by the ultrasound-guided intra-amniotic injection of IL-1α. The blockade of IL-6R by using an aIL-6R was tested as prenatal treatment for preterm birth and adverse neonatal outcomes. QUEST-MRI evaluated brain oxidative stress *in utero*. Targeted transcriptomic profiling assessed maternal, foetal, and neonatal inflammation. Neonatal biometrics and neurodevelopment were tested. The neonatal gut immune-microbiome was evaluated using metagenomic sequencing and immunophenotyping.**

Findings **IL-6 plays a critical role in the human intra-amniotic inflammatory response, which is associated with elevated concentrations of the alarmin IL-1α. Intra-amniotic injection of IL-1α resembles SIAI, inducing preterm birth (7% vs. 50%, p = 0.03, Fisher's exact test) and neonatal mortality (18% vs. 56%, p = 0.02, Mann–Whitney U-test). QUEST-MRI revealed no foetal brain oxidative stress upon *in utero* IL-1α exposure (p > 0.05, mixed linear model). Prenatal treatment with aIL-6R abrogated IL-1α-induced preterm birth (50% vs. 7%, p = 0.03, Fisher's exact test) by dampening inflammatory processes associated with the common pathway of labour. Importantly, aIL-6R reduces neonatal mortality (56% vs. 22%, p = 0.03, Mann–Whitney U-test) by crossing from the mother to the amniotic cavity, dampening foetal organ inflammation and improving growth. Beneficial effects of prenatal IL-6R blockade carried over to neonatal life, improving survival, growth, neurodevelopment, and gut immune homeostasis.**

*Corresponding author. Center for Reproductive Health Sciences, Washington University School of Medicine, BJC Institute of Health Rm 10618, 425 S. Euclid Avenue, St. Louis, MO, 63110, USA.
**Corresponding author. Pregnancy Research Branch, Division of Obstetrics and Maternal-Fetal Medicine, Division of Intramural Research, *Eunice Kennedy Shriver* National Institute of Child Health and Human Development, National Institutes of Health, Department of Health and Human Services (NICHD/NIH/DHHS), Bethesda, MD, USA.
E-mail addresses: nardhy@wustl.edu (N. Gomez-Lopez), romeror@mail.nih.gov (R. Romero).
[n]Authors contributed equally to this work.
The study was conducted at the Perinatology Research Branch, NICHD/NIH/DHHS, in Detroit, Michigan; the Branch has since been renamed as the Pregnancy Research Branch, NICHD/NIH/DHHS.

Interpretation IL-6R blockade can serve as a strategy to treat SIAI, preventing preterm birth and adverse neonatal outcomes.

Funding NICHD/NIH/DHHS, Contract HHSN275201300006C. WSU Perinatal Initiative in Maternal, Perinatal and Child Health.

Keywords: Alarmin; IL-1α; Microbiome; Pregnancy; Prematurity; Sterile intra-amniotic inflammation

Research in context

Evidence before this study

Prematurity remains as the leading cause of neonatal morbidity and mortality before five years of age globally. One in every three preterm infants is born to a pregnant individual with inflammation of the amniotic cavity (i.e., intra-amniotic inflammation), which is diagnosed by elevated concentrations of IL-6 in amniotic fluid. Most cases of intra-amniotic inflammation occur in the absence of microbes, a condition that was recently termed *sterile intra-amniotic inflammation*. Despite its prevalence and severe consequences, to date there is no approved treatment for this devastating obstetrical disease. Tocilizumab, an anti-IL-6 receptor monoclonal antibody, has been successfully utilised in pregnant individuals with inflammatory conditions such as rheumatoid arthritis. The recent COVID-19 pandemic further demonstrated the successful use of the anti-IL-6 receptor monoclonal antibody to reduce the inflammatory phase of infection caused by severe acute respiratory syndrome coronavirus-2 (SARS-CoV-2) in pregnant patients, with no reported detrimental maternal or foetal effects. Yet, treatment of sterile intra-amniotic inflammation with an anti-IL-6 receptor monoclonal antibody has not been investigated.

Added value of this study

We applied a multidisciplinary approach including human data together with the development of an animal model of sterile intra-amniotic inflammation-induced preterm birth to show that the blockade of IL-6R in the mother prevents preterm birth and mitigates adverse neonatal outcomes. Moreover, we demonstrated that the beneficial effects of prenatal IL-6 receptor blockade extend to neonatal life, thereby avoiding the long-term consequences of *in utero* exposure to sterile intra-amniotic inflammation for the health of the offspring.

Implications of all the available evidence

This study demonstrates the previously untested application of IL-6 receptor blockade for the prevention of preterm birth and adverse neonatal outcomes driven by sterile intra-amniotic inflammation. Importantly, our findings from this clinically relevant animal model provide a proof-of-concept for undertaking future studies in larger animals, and eventually humans, using aIL-6R to prevent preterm birth and adverse neonatal outcomes.

Introduction

Preterm birth (PTB) is the primary cause of mortality worldwide for children under five years of age.[1–3] Preterm neonates are at increased risk for a host of long-term consequences, including impaired growth and development during infancy[4–6] as well as multiple chronic diseases in adulthood.[7,8] Two out of three preterm deliveries are preceded by spontaneous preterm labour, a syndrome caused by multiple pathologic processes.[9,10] Among these, the best causal link to preterm labour and birth is intra-amniotic inflammation.[10–12] Clinically, intra-amniotic inflammation is diagnosed by elevated amniotic fluid concentrations of pro-inflammatory cytokines.[13–16] Such a local inflammatory response can be triggered by invading microorganisms (i.e., microbial intra-amniotic inflammation or intra-amniotic infection)[9,10,17–19] or by the release of endogenous danger signals, or alarmins, in the absence of microorganisms[20–22] (i.e., sterile intra-amniotic inflammation; hereafter referred to as SIAI).[20,23–27] Importantly, SIAI is more common than microbial intra-amniotic inflammation in patients with spontaneous preterm labour and intact membranes[20]; however, to date, there is no approved therapy to treat this obstetrical condition.[12]

The mechanisms of disease implicated in the intra-amniotic inflammatory response observed in patients with SIAI are still under investigation. A cytokine network analysis of amniotic fluid from patients with spontaneous preterm labour showed that the most interconnected node of cytokine interactions in patients with SIAI was led by interleukin (IL)-1α,[21] an alarmin that is causally linked to preterm birth.[28–30] Furthermore, the perturbation of intra-amniotic cytokines displayed by

patients with SIAI included a positive correlation between IL-1α and IL-6, the latter being a pleiotropic cytokine that can regulate the timing of parturition.[31,32] Indeed, IL-6 is the most reliable biomarker utilised to diagnose intra-amniotic inflammation in patients with spontaneous preterm labour.[13] Thus, IL-6 signalling is an ideal target for the treatment of SIAI and subsequent prevention of PTB; however, the potential utility of blocking or inhibiting this pathway has yet to be explored. Notably, antibody-mediated blockade of the IL-6 receptor (IL-6R) has been previously utilised as a treatment for pregnant patients with inflammatory conditions such as rheumatoid arthritis[33–35] or coronavirus disease-2019 (COVID-19).[36–41] Specifically, the anti-IL-6 receptor monoclonal antibody (aIL-6R) has been successfully used to reduce the inflammatory phase of infection caused by severe acute respiratory syndrome coronavirus-2 (SARS-CoV-2) with no reported detrimental maternal or foetal effects.[39–41] Previous studies in pregnant animals have utilised the administration of aIL-6R prior to[42] or at the same time as[43] the systemic administration of lipopolysaccharide (LPS), a model that resembles systemic inflammation. Such pre-treatment strategies require a reliable predictive disease model to ensure that prophylactic drugs are administered to the correct patients. Therefore, targeting the IL-6 pathway using aIL-6R has potential translational value and may be considered for the treatment of patients with SIAI to prevent preterm labour and birth and its related adverse neonatal outcomes.

In the current study, we employ data derived from human and murine samples to provide confirmatory evidence showing the critical role of IL-6 and IL-1α as key mediators of SIAI within the intraamniotic space. Next, we utilised a mouse model of SIAI induced by the intra-amniotic injection of IL-1α to investigate whether aIL-6R can serve as a treatment for the prevention of PTB and adverse neonatal outcomes. To evaluate the specificity of aIL-6R treatment for the prevention of PTB, a model of microbial intra-amniotic inflammation was also tested and contrasted with that of SIAI. In addition, foetal brain injury was evaluated using magnetic resonance imaging (MRI) in both animal models of PTB. Consequently, we mechanistically determined the effects of IL-6R blockade on the inflammatory responses in the maternal and foetal components of the common pathway of labour as well as in foetal organs involved in neonatal injury. Furthermore, the effects of prenatal treatment with aIL-6R on neonatal outcomes, including neurodevelopment and intestinal immune-microbiome interactions, were also evaluated using neuromotor assessment, metagenomic sequencing, and immunophenotyping. Overall, this study provides a mechanistic investigation supporting the use of aIL-6R as a potential therapy for preventing PTB and adverse neonatal outcomes induced by SIAI, offering an intervention for a clinical condition with no current treatment.

Methods

Animals

C57BL/6 (strain #000664) mice were purchased from The Jackson Laboratory (Bar Harbor, ME, USA) and housed in the animal care facility at the C.S. Mott Center for Human Growth and Development at Wayne State University (Detroit, MI, USA). Mice were kept under a circadian cycle (light:dark = 12:12 h) with environmental enrichment consisting of nesting squares and plastic igloos. Eight-to 12-week-old female C57BL/6 mice were mated with males of proven fertility. Females were checked daily (8–9 a.m.) to detect the presence of a vaginal plug, which indicated 0.5 days *post coitum* (dpc). Plugged females were then housed separately, and their weights were monitored daily. A weight gain of ≥2 g by 12.5 dpc confirmed pregnancy. The study objective was to determine whether the blockade of IL-6R using a monoclonal antibody could prevent PTB and adverse neonatal outcomes in a mouse model of alarmin-induced intra-amniotic inflammation. Research subjects were pregnant mice and their offspring. All mice were randomly assigned to the different treatment or control groups (described below), and investigators were not masked to the group assignment. Numbers of biological replicates are indicated in each figure legend. Power analysis was performed based on the rate of preterm birth induced by IL-1α compared to controls previously established by our group,[30] resulting in a power of 0.68. Based on these data, a sample size of n = 6 mice per group would be necessary to achieve a power of 0.8. The minimal number of mice was considered, following the "Three Rs" for animal use alternatives.[44]

Single-cell RNA sequencing (scRNA-seq) analysis of the human placental tissues

Publicly available scRNA-seq data were used to explore the expression of *IL6* in the human chorioamniotic membranes. Briefly, raw fastq files were downloaded from previously established resources in NCBI dbGaP phs001886.v1.p1.[45] The fastq files were then aligned using kallisto,[46] and bustools[47] summarised the cell/gene transcript counts in a matrix for each sample using the "lamanno" workflow for scRNA-seq. Each sample was then processed using DIEM[48] to eliminate debris and empty droplets. All count data matrices were then normalised and combined using the "NormalizeData," "FindVariableFeatures," and "ScaleData" methods implemented in the Seurat package in R (Seurat v3.1, R v3.6.1).[49,50] Afterward, the Seurat "RunPCA" function was applied to obtain the first 50 principal components, and the different batches and locations were integrated and harmonised using the Harmony package in R.[51] The top 30 harmony components were then processed using the Seurat "runUMAP" function to embed and visualise the cells in a two-dimensional map via the Uniform Manifold Approximation and Projection (UMAP)

algorithm for dimension reduction. To label the cells, the Seurat "FindTransferAnchors" and "TransferData" functions were used for each group of locations separately to assign a cell type identity based on our previously labeled data as reference panel (as performed in[45]). We used only the subset of samples from the chorioamniotic membranes of patients who underwent term labour (TIL) or preterm labour (PTL) (n = 3 per group). Normalisation of gene expression of *IL6* for each cell type was scaled to transcripts per million (TPM), and only the subset of cells that expressed *IL6* were used in the boxplots.

Single-cell RNA sequencing (scRNA-seq) analysis of gestational tissues in a mouse model of preterm labour

Publicly available scRNA-seq data were used to explore the expression of *Il6* in the uterus, decidua, and cervix of a mouse model of preterm labour.[52] The processed Seurat object was downloaded from GEO accession number GSE200289. The same cell type labelling and UMAP coordinates were used as reported in our previous study (Garcia-Flores et al., 2023).[52] We visualised the UMAP plot while showing the expression levels for *Il6* for the three tissues combined, contrasting the two conditions: preterm labour/birth mice compared to controls (n = 4 per group). Normalisation of gene expression for each cell type was scaled to transcripts per million (TPM) and $\log_{10}$ (1 + x) transformed.

Intra-amniotic administration of IL-1α or LPS

Ultrasound-guided intra-amniotic injection of IL-1α (Cat# 200-LA/CF; R&D Systems, Minneapolis, MN, USA) or LPS (Cat# L4391; *Escherichia coli* O111:B4; Sigma–Aldrich, St. Louis, MO, USA) were used to model sterile or microbial intra-amniotic inflammation in mice, respectively, as previously reported.[30,53–56] Briefly, dams were anesthetised at 16.5 dpc by inhalation of 1.75–2% isoflurane (FlurisoTM/Isoflurane, USP; VetOne, Boise, ID, USA). Mice were positioned on a heating pad and stabilised with adhesive tape, and fur was removed from the abdomen using Nair cream (Church & Dwight Co., Inc., Ewing, NJ, USA) as previously described.[57] Dams were intra-amniotically injected with IL-1α at concentrations of 10, 20, 25, or 50 ng dissolved in 25 μL of sterile 1X phosphate-buffered saline (PBS; Fisher Scientific Bioreagents, Fair Lawn, NJ, USA or Life Technologies Limited, Paisley, UK) or LPS at concentrations of 100 ng dissolved in 25 μL of sterile PBS in each amniotic sac under ultrasound guidance using the Vevo® 2100 Imaging System (VisualSonics Inc., Toronto, Ontario, Canada) and a 30G needle (BD PrecisionGlide Needle, Becton Dickinson, Franklin Lakes, NJ, USA). Control dams were intra-amniotically injected with 25 μL of PBS. Successful intra-amniotic injection was confirmed by using colour Doppler ultrasound to identify the "injection jet sign".[58,59] Following intra-amniotic injection, mice were placed under a heat lamp until recovery, which was typically 5–10 min after removal from anaesthesia.

Anti-IL-6 receptor (aIL-6R) blockade

Six h after injection with IL-1α or LPS, pregnant mice were intra-peritoneally injected with the anti-IL-6 receptor (aIL-6R; 10 mg/kg) monoclonal antibody (InvivoMab rat anti-mouse IL-6R, clone 15A7, Cat# BE0047, Bio X Cell Inc, Lebanon, NH, USA) or IgG2b isotype (10 mg/kg) as control (InVivoMAb rat IgG2b isotype control, anti-keyhole limpet hemocyanin, clone LTF-2, Cat# BE0090, Bio X Cell Inc). The 6 h timepoint was chosen based on our previous work showing that PTB can be prevented by an anti-inflammatory drug in a model of systemic inflammation.[60]

Video monitoring of perinatal outcomes

Primary observational outcomes included the rates of PTB and neonatal mortality, which were recorded with a video camera system (Sony Corporation, Tokyo, Japan). Gestational length was calculated as the time from the presence of the vaginal plug (0.5 dpc) until the detection of the first pup in the cage bedding. Preterm birth was defined as delivery before 18.5 dpc. The rate of PTB was calculated as the proportion of females delivering preterm out of the total number of mice per group. The rate of neonatal mortality was defined as the proportion of delivered pups found dead among the total number of pups.

Neonatal outcomes

Neonatal survival and weights were monitored weekly until postnatal day (PND) 21. Head biparietal diameter was measured at week 3 by using a digital calliper (Chemglass Life Sciences, Vineland, NJ, USA). Neuromotor behaviour was examined on the morning of PND 5 and included the following tests: surface righting, negative geotaxis, and cliff aversion. For the surface righting test, each pup was placed on its back on a flat table, and the ability and time required to flip onto its feet from a supine position were recorded (maximum time 60 s). For the negative geotaxis test, each pup was placed on a board inclined at a 45° angle with the head pointing downwards, and the ability and time required to turn 180° with the head, trunk, and forepaws facing upwards were recorded (maximum time 120 s). For cliff aversion, pups were placed on a cliff with forepaws over the edge, and the ability and time to turn at least 90° away from the edge were recorded (maximum time 30 s).[61,62]

QUEST MRI-based detection of elevated free radical production in the foetal brain

Six h after intra-amniotic injection with LPS or IL-1α, dams were intraperitoneally injected with 10 mg/kg of rosiglitazone (ROSI, Cat# S2556, Selleckchem,

Houston, TX, USA) dissolved in 200 μL of sterile PBS, as previously reported.[63] QUEnch-assiSTed magnetic resonance imaging (QUEST MRI) was performed 9–10 h after injection with ROSI similar to a procedure previously described.[63] Briefly, high-resolution T1 relaxation rate (R1) data were acquired on a 7T system (Bruker BioSpec AV4 Neo, Billerica, MA, USA), using a commercial receive-only surface coil (1.0 cm diameter) that was part of the coil set for the BioSpec. In all cases, several single spin-echo (time to echo [TE] 13 ms, 7 × 7 mm^2, matrix size 160 × 320, slice thickness 600 μm, in-plane resolution 21.875 μm) images were acquired. Different repetition times (TRs) were used in the following order (number of scans per TR in parentheses): TR 0.15 s (6), 3.50 s (1), 1.00 s (2), 1.90 s (1), 0.35 s (4), 2.70 s (1), 0.25 s (5), and 0.50 s (3). To compensate for reduced signal:noise ratios at shorter TRs, progressively more images were collected for averaging as the TR decreased. The slice chosen for these studies has been previously demonstrated.[63] Note that the BioSpec system did not acquire data by motion-correction sequences such as periodically rotated overlapping parallel lines with enhanced reconstruction (i.e., BLADE) as had been utilised in earlier work.[63] Instead, data were collected using a conventional spin-echo sequence, which has been previously demonstrated to work well for R1 mapping in QUEST-MRI studies of the retina.[64] To help mitigate motion artifacts, dams were anesthetised with an intraperitoneal injection of urethane (2.3 g/k of animal weight, diluted in PBS, Sigma–Aldrich, Cat# U2500) instead of isoflurane, an anaesthetic that produces gasping.[65] In addition, we collected several single spin-echo (time to echo [TE] 11.17 ms, 17 × 17 mm^2, matrix size 128 × 128, slice thickness 400 μm, in-plane resolution 133 μm) images in two phase-encode directions; these two sets of data were compared and/or averaged, which suppressed motion artifacts in the final R1 image. As before, a foetus was gently immobilised *in utero* using a 3D-printed clip designed for this purpose, as previously described.[63] An abnormal, continuous production of paramagnetic free radicals (indicative of oxidative stress) in the left and right brain hemispheres (combined caudate-putamen and thalamus region of interest) was inferred from the difference in an R1 signal between ROSI-treated (a drug with antioxidant properties[66]) and non-treated dams.[63] Therefore, a decrease in an R1 signal upon ROSI treatment was considered indicative of foetal brain oxidative stress.

We used a linear mixed model to analyse R1, conducting separate analyses for the mice from LPS-injected vs. IL1α-injected dams. The model included the fixed effect of treatment (ROSI vs. control), side, and the treatment by side interaction as well as a random intercept for each mouse within treatment. Degrees of freedom were calculated using the Kenward-Roger method. The treatment by side interaction was not significant so the interaction was removed to obtain the final model, and this model was used to calculate R1 differences averaged across the site. Results are presented as means with 95% confidence intervals, and we used a 5% significance level for all tests. All analyses were conducted using Proc Mixed of SAS v9.4 (SAS software, Cary, NC, USA).

Sampling of maternal–foetal tissues

Pregnant mice received an intra-amniotic injection of IL-1α or PBS on 16.5 dpc and 6 h after were intraperitoneally injected with aIL-6R or isotype antibodies, as described above. Mice were euthanised at 17.5 dpc (16 h after the initial injection, before PTB), and animal dissection was performed for tissue collection. The amniotic fluid was collected from each amniotic sac and centrifuged at 1300×*g* for 5 min at 4 °C. The resulting supernatants were stored at –20 °C until analysis. After dissection of the uterine horns, the vaginal border was carefully removed, and the upper limit of the cervix was incised to isolate the cervical tissue. Pictures and macroscopic measurements of cervical length and width were obtained as surrogates of cervical modifications associated with labour, as previously described.[56,67] The uterus, decidua, placenta, foetal membranes, foetal brain, foetal lung, and foetal intestine were also collected. Pictures and weights of the placentas and foetuses were obtained during animal dissection. The collected tissues were preserved in RNA*later* Stabilization Solution (Cat# AM7021; Invitrogen by Thermo Fisher Scientific, Carlsbad, CA, USA), according to the manufacturer's instructions, and stored at –80 °C for reverse transcription-quantitative polymerase chain reaction (RT-qPCR).

Sampling of neonatal tissues

Pregnant mice received an intra-amniotic injection of IL-1α or PBS on 16.5 dpc and 6 h after were intraperitoneally injected with aIL-6R or isotype antibodies, as described above. Dams were allowed to deliver, and neonates were monitored for adverse outcomes in the first three weeks of life. All neonatal samples were obtained at PND 21. Thriving neonates were euthanised, and the brain, lung, colon, caecum, and small intestine were collected, rinsed in PBS, and stored for molecular determinations. For RNA studies, the neonatal brain, lung, colon, caecum, and small intestine were placed into RNA*later* Stabilization Solution, according to the manufacturer's instructions. For leukocyte isolation and immunophenotyping, samples from the neonatal colon, caecum, and small intestine were placed in cold PBS before processing. For microbiome studies, samples from the neonatal colon, caecum, and small intestine, as well as environmental controls, were obtained using sterile swabs (FLOQSwabs, Cat# 553C Copan Diagnostics, Murieta, CA, USA) under aseptic conditions.

Detection of maternal–foetal transfer of aIL-6R

Fluorescence labelled aIL-6R antibody was prepared using the Alexa Fluor™ 647 antibody labelling kit (Cat# A20186, Molecular Probes, ThermoFisher Scientific, Waltham, MA, USA), following the manufacturer's instructions. Pregnant mice (n = 5) were intra-amniotically injected with IL-1α and 6 h after were intraperitoneally injected with the Alexa Fluor™647-conjugated aIL-6R antibody (10 mg/kg). The following day, the uterine horns were collected for imaging using the *in vivo* imaging system (IVIS, Caliper Life Sciences, Hopkinton, MA, USA) in epi-fluorescence mode. Next, the amniotic fluid and maternal plasma were collected to determine the concentration of Alexa Fluor™647-conjugated aIL-6R antibody by fluorescence quantification using the SpectraMax iD5 multi-mode microplate reader (Molecular Devices, San Jose, CA, USA).

Cytokine determinations in amniotic fluid

Amniotic fluid samples were analysed for IL-6, IL-1β, and TNF concentrations using the U-PLEX Custom Biomarker Group 1 (mouse) assay (Cat# K15069L Meso Scale Discovery, Rockville, MD, USA), according to the manufacturer's instructions. Assay plates were read using the MESO QuickPlex SQ 120 (Meso Scale Discovery), and analyte concentrations were calculated using the Discovery Workbench software v4.0 (Meso Scale Discovery). The lower limit of detection (LLOD) for each analyte was 4.8 pg/mL (IL-6), 3.1 pg/mL (IL-1β), and 1.3 pg/mL (TNF).

Gene expression determination

Total RNA was isolated from the uterus, decidua, cervix, placenta, foetal membranes, foetal lung, foetal brain, neonatal lung, neonatal brain, neonatal small intestine, neonatal colon, and neonatal caecum using QIAshredders (Cat# 79656; Qiagen, Hilden, Germany), RNase-Free DNase Sets (Cat# 79254; Qiagen), and RNeasy Mini Kits (Cat# 74106; Qiagen), according to the manufacturer's instructions. A NanoDrop 8000 spectrophotometer (Thermo Scientific, Wilmington, DE, USA) and a Bioanalyzer 2100 (Agilent Technologies, Waldbronn, Germany) were used to evaluate RNA concentrations, purity, and integrity. SuperScript IV VILO Master Mix (Cat# 11756050; Invitrogen by Thermo Fisher Scientific Baltics UAB, Vilnius, Lithuania) was used to synthesise complementary DNA. Gene expression profiling of the tissues was performed on the BioMark System for high-throughput RT-qPCR (Fluidigm, San Francisco, CA, USA) with the TaqMan gene expression assays (Applied Biosystems, Life Technologies Corporation, Pleasanton, CA, USA) listed in Table S1. Negative delta cycle threshold ($-\Delta C_T$) values were determined using multiple reference genes (*Actb*, *Gapdh*, *Gusb*, and *Hsp90ab1*) averaged within each sample.

Characterisation of the neonatal gut microbiome

DNA extraction

Genomic DNA was extracted from previously collected swabs of the small intestine, caecum, and colon (n = 44 each) alongside non-template negative controls (n = 13) to address any potential background DNA contamination. Only one of those controls yielded a metagenomic library. By contrast, all small intestine and caecum samples yielded a metagenomic library while 36 colon samples yielded a metagenomic library. All swabs were randomised across extraction runs. Extractions were conducted using a Qiagen MagAttract PowerMicrobiome DNA/RNA EP extraction kit (Qiagen, Germantown, MD, USA) and an epMotion 5075 liquid handler (Eppendorf, Enfield, CT, USA). The purified DNA was transferred to 96-well microplates and stored at –20 °C.

Metagenomic sequencing

DNA samples underwent metagenomic sequencing using the Illumina NovaSeq 6000 S4 150-base paired-end read protocol at the University of Michigan's Advanced Genomics Core. Prior to taxonomic and functional classification of the intestinal metagenomic sequence reads, raw reads were subjected to adapter removal and were quality-trimmed using bbduk[68] with the following options: qtrim = rl, trimq = 21, minlength = 100, tpe, and tbo. Taxonomic classification of bacterial sequence reads was performed using Kraken 2.1.2[69] and the Kraken PlusPFP database with the following options: minimum-hit-groups = 2 and confidence = 0.3. Abundance estimation was performed with Bracken v2.6[70] based on a read length of 150 bp and a kmer length of 35. Of the 300 bacterial species identified, two species were removed from the dataset because they had greater relative abundances in the non-template negative control sample than in the biological samples (*Staphylococcus aureus* 45.7% > 0.07%; *Cupriavidus metallidurans* 19.7% > 4.78%). All small intestine samples were normalised to 50,466 reads, and all caecum and colon samples were normalised to 1,278,327 reads using the "rarefy_even_depth" function in phyloseq 1.42.0,[71] resulting in 42, 44, and 36 bacterial profiles for each of the three sample types, respectively. No cross-tissue comparisons were conducted.

Bacterial community analysis

Alpha diversity metrics (Chao1, Shannon, and Inverse Simpson) of bacterial profiles were calculated with phyloseq 1.42.0.[71] Differences in alpha diversity index values between treatments were assessed for each tissue type using Mann–Whitney U-tests. Beta diversity of bacterial profiles was characterised using the Bray–Curtis similarity index. Bray–Curtis similarity of sample profiles was visualised using principal coordinate analysis (PCoA) plots. Differences in bacterial community structure between treatments were assessed for each tissue type using nonparametric multivariate

analysis of variance (NPMANOVA) within the R vegan 2.6.4 package. Given the difference in a bacterial read count generated for the small intestine samples compared to the caecum and colon samples, only the latter two sample types were considered for assessing differential abundance of individual bacterial taxa between treatment groups. For both the caecum and colon datasets, the relationship between the 25 most abundant bacterial species between treatment groups was independently assessed using Mann–Whitney U-tests with Holm's correction for multiple comparisons as implemented in R v4.2.2. Adjusted p-values <0.1 were considered significant.

Leukocyte isolation from neonatal tissues

Isolation of leukocytes for immunophenotyping from the neonatal colon, caecum, and small intestine were performed as previously reported with some modifications.[54] Briefly, the neonatal colon, caecum, and small intestine were collected from three neonates of the same litter and pooled per experiment (n = 6–10 each). Tissues were gently minced using fine scissors and enzymatically digested with StemPro Accutase Cell Dissociation Reagent (Cat# A1110501, Thermo Fisher) for 15 min at 37 °C. Leukocyte suspensions were filtered using a 100 μm cell strainer (Cat# 22-363-549, Fisher Scientific, Fair Lawn, NY, USA), followed by washing with PBS prior to immunophenotyping.

Immunophenotyping of leukocytes from neonatal tissues

Leukocyte suspensions from the neonatal tissues were stained using LIVE/DEAD Fixable Viability Stain (BD Biosciences, San Jose, CA, USA) prior to incubation with extracellular and intracellular mAbs. Leukocyte suspensions were centrifuged at 1250×*g* for 7 min at 4 °C and then incubated with specific fluorochrome-conjugated monoclonal antibodies (Table S2) for 30 min at 4 °C. After washing, the cells were fixed and permeabilised with the FOXP3/Transcription Factor Staining Buffer set (Cat# 00-5523-00; Thermo Fisher) for 30 min at 4 °C. Next, the cells were incubated with anti-mouse antibodies for intracellular markers (Table S2) for 30 min at 4 °C. The cells were acquired using the BD LSRFortessa flow cytometer (BD Biosciences) with FACSDiva 9.0 software (BD Biosciences). The analysis and preparation of images were performed using FlowJo Software v10 (Tree Star, Ashland, OR, USA).

Statistics

Observational, gene expression, and flow cytometry data were analysed with GraphPad Prism v9 (v9.0.2; GraphPad, San Diego, CA, USA). For observational data, the Fisher's exact test and the two-tailed Mann–Whitney U-test were used to compare the rates of PTB and neonatal mortality, respectively, between two study groups (PBS/Isotype vs. IL-1α/Isotype, or IL-1α/Isotype vs. IL-1α/aIL-6R). Kaplan–Meier survival curves were used to plot and compare the gestational length data, with the start of follow-up at 16.5 dpc, the end of follow-up at 21 dpc, and the delivery of the first pup as the censoring point. A Gehan-Breslow-Wilcoxon test was used to evaluate differences between the survival curves from two groups (PBS/Isotype vs. IL-1α/Isotype; or IL-1α/Isotype vs. IL-1α/aIL-6R). To determine gene expression levels from RT-qPCR arrays, $-\Delta C_T$ values were calculated using averaged reference genes (*Actb, Gapdh, Gusb*, and *Hsp90ab1*) within each sample. Heatmaps were created to represent the Z-scores of the mean ($-\Delta C_T$), ordered by highest to lowest degree of gene expression using the IL-1α/Isotype group as a reference. Similarly, for flow cytometry data, heatmaps were created to represent the Z-score of the mean (cell population frequencies), ordered by highest to lowest subpopulation frequencies using the IL-1α/Isotype group as a reference. For individual plots, two-tailed Mann–Whitney U-tests was utilised to compare between two groups. A p-value <0.05 was considered significant. QUEST MRI data were analysed using Proc Mixed of SAS 9.4, as described above. General microbiome data analysis was performed using R (v.4.2.2; https://www.r-project.org/), as described above.

Ethics

The reanalysis of human amniotic fluid proteins and scRNA-seq data was performed using available de-identified datasets. These samples were taken after obtention of written informed consent, and ethical approval was obtained from the Institutional Review Boards of Wayne State University (Detroit, MI, USA) and/or the National Institute of Child Health and Human Development (NICHD)/National Institutes of Health/U.S. Department of Health and Human Services (Bethesda, MD, USA).[21,22,45]

All animal experimental procedures were performed in compliance with guidelines set by the Institutional Animal Care and Use Committee (IACUC) at Wayne State University under Protocol 21-04-3506. The methods are reported in accordance with ARRIVE guidelines for the reporting of animal experiments.

Role of funders

The funders had no role in the study design, data collection and interpretation, or the decision to submit the work for publication.

Results

Blockade of IL-6R protects against preterm birth and neonatal mortality induced by IL-1α

SIAI is defined as the presence of an elevated concentration of IL-6 in the absence of detectable bacteria, as demonstrated by both conventional and molecular

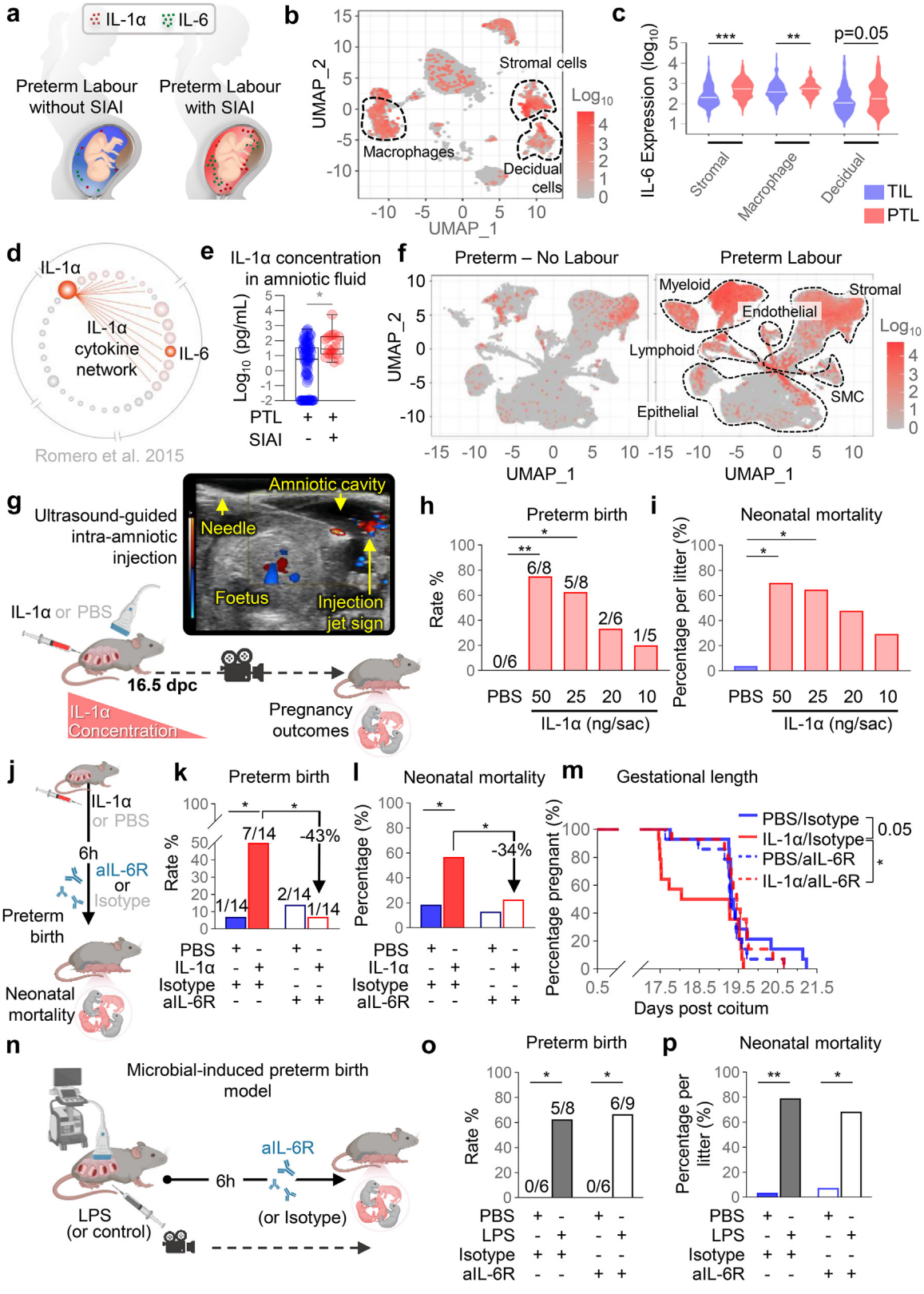
a
IL-1α
IL-6
Preterm Labour without SIAI
Preterm Labour with SIAI
b
Stromal cells
Macrophages
Decidual cells
Log10
UMAP_2
UMAP_1
c
IL-6 Expression (log10)
***
**
p=0.05
Stromal
Macrophage
Decidual
TIL
PTL
d
IL-1α
IL-1α cytokine network
IL-6
Romero et al. 2015
e
IL-1α concentration in amniotic fluid
Log10 (pg/mL)
PTL
SIAI
f
Preterm – No Labour
Preterm Labour
Myeloid
Stromal
Endothelial
Lymphoid
SMC
Epithelial
g
Ultrasound-guided intra-amniotic injection
Amniotic cavity
Needle
Foetus
Injection jet sign
IL-1α or PBS
16.5 dpc
IL-1α Concentration
Pregnancy outcomes
h
Preterm birth
Rate %
6/8
5/8
2/6
1/5
0/6
PBS
IL-1α (ng/sac)
i
Neonatal mortality
Percentage per litter (%)
j
IL-1α or PBS
6h
aIL-6R or Isotype
Preterm birth
Neonatal mortality
k
Preterm birth
7/14
-43%
2/14
1/14
1/14
PBS
IL-1α
Isotype
aIL-6R
l
Neonatal mortality
-34%
m
Gestational length
Percentage pregnant (%)
PBS/Isotype
IL-1α/Isotype
PBS/aIL-6R
IL-1α/aIL-6R
0.05
*
Days post coitum
n
Microbial-induced preterm birth model
aIL-6R
6h
LPS (or control)
(or Isotype)
o
Preterm birth
5/8
6/9
0/6
0/6
LPS
Isotype
aIL-6R
p
Neonatal mortality

microbiologic techniques (Fig. 1a).[20,25,26] Therefore, in this study, we initially utilised our previously generated single-cell RNA sequencing (scRNA-seq) data from human chorioamniotic membranes[45] (the extraembryonic tissues surrounding the amniotic cavity) to investigate potential sources of IL-6 in the intra-amniotic space. Our findings revealed that multiple cell types within the chorioamniotic membranes express *IL6* (Fig. 1b). Notably, the expression of *IL6* by stromal, macrophage, and decidual cell types was found to be higher in preterm labour cases compared to term labour controls (Fig. 1c), suggesting the involvement of the chorioamniotic membranes in IL-6 expression driven by intra-amniotic inflammation. Next, we revisited a previously reported cytokine network analysis of the amniotic fluid of patients with preterm labour and SIAI[21] and found that the IL-1α module is enriched in the amniotic cavity of patients with preterm labour and SIAI (Fig. 1d). Indeed, the amniotic fluid concentrations of IL-1α are elevated in patients with SIAI compared to those without SIAI (Fig. 1e). Furthermore, the concentrations of this alarmin were correlated with those of multiple pro-inflammatory mediators,[21] including IL-6 (Fig. 1d), the canonical marker of intra-amniotic inflammation.[13] Interestingly, using available scRNA-seq data from a murine model of preterm labour and birth, as evidenced by sonographic cervical shortening,[52] we found that *Il6* is consistently upregulated in multiple cell types in labour-associated tissues (e.g., uterus and decidua) from mice undergoing preterm labour compared to preterm no labour controls (Fig. 1f, Table S3). Specifically, *Il6* expression was increased in the macrophage, stromal, epithelial, fibroblast, and monocyte cell clusters from both the decidua and myometrium as well as in endothelial and smooth muscle cell clusters from the myometrium of mice undergoing preterm labour (Table S3).

By utilizing previous knowledge generated in our laboratory, we performed animal experimentation to establish a model of PTB induced by SIAI that resembled the clinical scenario. Approximately 50% of patients diagnosed with preterm labour, SIAI, and elevated intra-amniotic concentrations of alarmins undergo PTB within one week[20]; therefore, we tested several intra-amniotic concentrations of IL-1α to determine whether they cause delivery within 24–48 h post-injection (Fig. 1g). Intra-amniotic administration of IL-1α induced PTB and neonatal mortality in a dose-dependent manner (Fig. 1h and i). The intra-amniotic injection of 25 ng of IL-1α induced PTB in 60% of cases; therefore, this dose was chosen for further studies. Subsequently, we investigated whether the blockade of IL-6R could protect against PTB and neonatal mortality induced by intra-amniotic IL-1α (Fig. 1j). Notably, the blockade of IL-6R abrogated the adverse perinatal outcomes induced by IL-1α, reducing the rates of PTB and neonatal mortality by 43% (Fig. 1k) and 34% (Fig. 1l), respectively. Consequently, treatment with aIL-6R extended the gestational length of dams injected with IL-1α to resemble that of control dams (Fig. 1m). These results demonstrate that the blockade of IL-6R can prevent PTB and neonatal mortality induced by elevated intra-amniotic concentrations of the alarmin IL-1α (i.e., SIAI).

Previous studies have suggested that treatment of microbial-driven inflammation-related PTB could be

***Fig. 1:* Blockade of IL-6R reduces preterm birth and neonatal mortality induced by IL-1α.** **(a)** Schematic representation showing the increased amniotic fluid concentrations of the alarmin IL-1α and the biomarker of intra-amniotic inflammation, IL-6, in patients with sterile intra-amniotic inflammation (SIAI). **(b)** Uniform Manifold Approximation and Projection (UMAP) plot showing the expression of *IL6* by cell types in the chorioamniotic membrane of patients who underwent spontaneous term or preterm labour (n = 3 per group). Dotted lines represent cell clusters with the highest *IL6* expression. **(c)** Violin plots represent the expression of *IL6* by the Stromal, Macrophage, and Decidual cell clusters compared between patients who underwent spontaneous term (TIL) or preterm (PTL) labour. **(d)** IL-1α module of cytokine network interactions in the amniotic fluid of pregnant patients with preterm labour and SIAI (modified from Romero et al. 2015). **(e)** Amniotic fluid concentrations of IL-1α (pg/mL) in pregnant patients with preterm labour with or without SIAI (modified from Bhatti et al. 2020). Data are shown as box-and-whisker plots where midlines indicate medians, boxes indicate interquartile ranges, and whiskers indicate minimum and maximum values. **(f)** UMAP plots showing the expression of *Il6* by cell types in labour-associated tissues from control (preterm no labour) mice (left panel) or mice undergoing preterm labour (right panel; n = 4 per group). Dotted lines represent cell clusters with the highest *Il6* expression. SMC, smooth muscle cell. **(g)** Experimental model for the induction of SIAI by ultrasound-guided intra-amniotic injection of IL-1α (or PBS control) on 16.5 days *post coitum* (dpc), with successful injection confirmed by observation of the "injection jet sign" by using colour Doppler ultrasound. **(h)** Preterm birth and **(i)** neonatal mortality rates in mice injected with PBS (blue, n = 6 litters) or IL-1α (light red, n = 5–8 litters per group). **(j)** Experimental design for treatment of IL-1α- or PBS-injected dams with rat anti-mouse IL-6 receptor monoclonal antibody (aIL-6R) or rat IgG2b isotype (control) 6 h after intra-amniotic injection. **(k)** Preterm birth and **(l)** neonatal mortality of dams injected with PBS/Isotype (filled blue bars), IL-1α/Isotype (filled red bars), PBS/aIL-6R (open blue bars), and IL-1α/aIL-6R (open red bars) (n = 14 per group). **(m)** Gestational lengths of dams from the four experimental groups displayed as Kaplan–Meier survival curves (n = 14 dams at risk per group). **(n)** Model of microbial-induced preterm birth and treatment with aIL-6R or isotype. **(o)** Preterm birth and **(p)** neonatal mortality were evaluated in mice injected with PBS/Isotype (filled blue bars), LPS/Isotype (filled black bars), PBS/aIL-6R (open blue bars), and LPS/aIL-6R (open black bars) (n = 6–9 litters per group). Data are shown as bar plots. p-values were determined using the Fisher's exact test for preterm birth rate, two-sided Mann–Whitney U-tests for neonatal mortality, and the Gehan-Breslow-Wilcoxon test for Kaplan–Meier survival curve comparisons. *p < 0.05; **p < 0.01; ***p < 0.001.

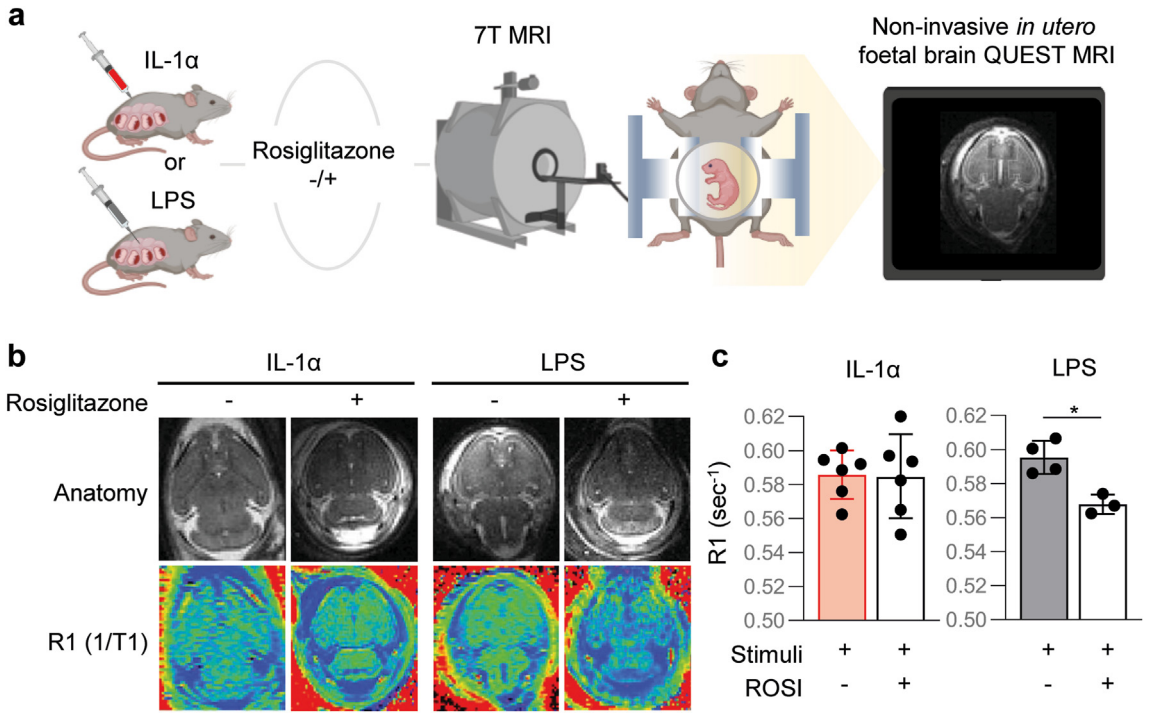

Fig. 2: **Differential effect of sterile and microbial intra-amniotic inflammation on an MRI imaging biomarker of free radical production/oxidative stress in the foetal brain.** **(a)** Left: Dams were intra-amniotically injected with IL-1α (25 ng/25 μL per sac) or LPS (100 ng/25 μL per sac). Six h later, a portion of dams from each group received an intraperitoneal injection of rosiglitazone (ROSI; 10 mg/kg), and all dams underwent *in utero* MRI scanning using a 7T system. Continuous production of paramagnetic free radicals (indicative of oxidative stress) in the region of interest (ROI) located in the left and right brain hemispheres was inferred from the difference in the R1 (=1/T1) signal between ROSI-treated (a drug with antioxidant properties) and untreated dams. Right: Representative image showing the foetal brain. **(b)** Top row: Representative anatomical images (generated by normalizing the TR 150 ms image) for each study group. Bottom row: Corresponding R1 maps. All images were fixed to the same scale with darker colours indicating lower R1 values. **(c)** Modelled mean of the ROI R1 from both hemispheres of either IL-1α and IL-1α + ROSI groups (left bar graph, n = 6 per group) or LPS and LPS + ROSI groups (right bar graph, n = 3–4 per group). Data are presented as means and confidence intervals. p-values were determined using linear mixed modelling. *p < 0.05.

achieved by blocking or inhibiting general inflammatory pathways. Yet, we challenged this view since blocking key components of the innate immune system (e.g., the inflammasome) consistently worsened adverse perinatal outcomes upon administration of intra-amniotic bacteria (Gomez-Lopez et al., unpublished data). Thus, we propose that treatments for PTB should be tailored to the nature of the inflammatory response, resulting in therapies for SIAI that may not be useful to prevent microbial intra-amniotic inflammation and vice versa. To evaluate this concept, we used our animal model of LPS-induced intra-amniotic inflammation, an experimental approach to model microbial-induced PTB[53–56] (Fig. 1n). Intra-amniotic injection of LPS induced high rates of PTB and neonatal mortality; however, treatment with aIL-6R did not prevent such adverse perinatal effects (Fig. 1o and p). To dive deeper into the divergent inflammatory responses induced by alarmins and microbial products, we tested for the continuous and asynchronous production of paramagnetic free radicals as a proxy for foetal brain oxidative stress using *in utero* QUEST MRI combined with rosiglitazone (ROSI), an antioxidant used as the quenching agent[63] (Fig. 2a). As previously established,[63] the foetuses of dams intra-amniotically injected with LPS displayed signs of foetal brain oxidative stress; however, this phenomenon was not observed in foetuses of dams intra-amniotically injected with IL-1α (Fig. 2b and c). These findings indicate that the blockade of IL-6R serves to treat SIAI and prevent the resulting PTB, but not that induced by microbial signals (i.e., LPS), highlighting the distinct nature of these two intra-amniotic inflammatory responses and emphasizing that different therapeutic strategies should be utilised for each clinical condition.

Blockade of IL-6R interferes with the common pathway of labour

Next, we investigated the mechanisms whereby the blockade of IL-6R prevents PTB. The processes of term and preterm labour share a common pathway that precedes the delivery of the offspring.[72–75] Such a pathway includes uterine contractility, cervical remodelling, and

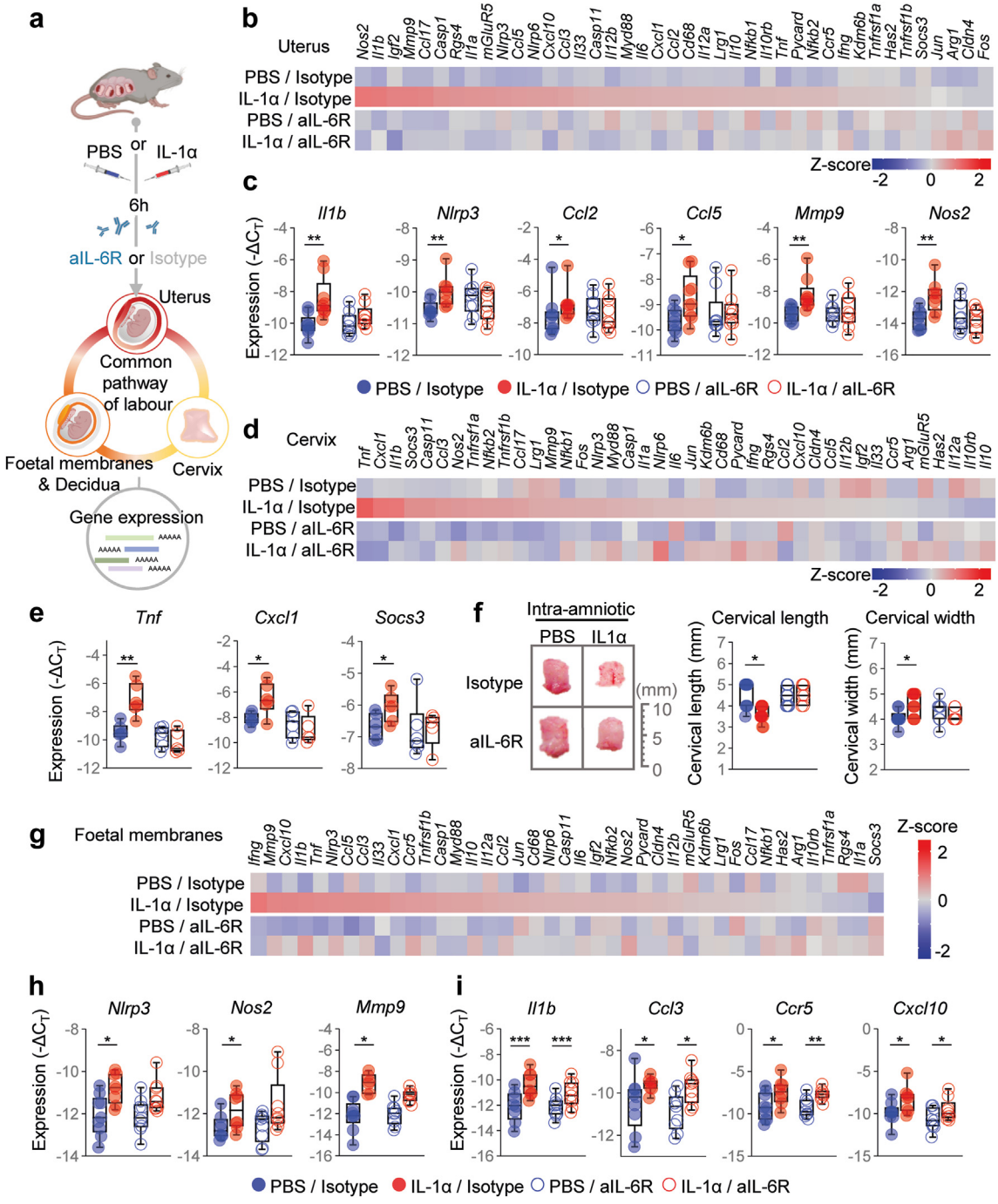

***Fig. 3:* Blockade of IL-6R interferes with the common pathway of labour induced by intra-amniotic IL-1α.** **(a)** Dams underwent intra-amniotic injection of PBS (control) or IL-1α on 16.5 days *post coitum* (dpc). Six h later, dams were intra-peritoneally injected with rat anti-mouse IL-6 receptor monoclonal antibody (aIL-6R) or rat IgG2b isotype (control). Sixteen h after the intra-amniotic injection, the uterus, cervix, foetal membranes, and decidua were collected to analyse gene expression by directed high-throughput RT-qPCR. **(b)** Heatmap representation of inflammatory gene expression in the uterine tissue (n = 9 per group). Red indicates increased expression and blue indicates decreased expression. **(c)** Gene expression ($-\Delta C_T$) of *Il1b*, *Nlrp3*, *Ccl2*, *Ccl5*, *Mmp9*, and *Nos2* in the uterus. **(d)** Heatmap representation of inflammatory gene expression in the cervix (n = 9 per group). **(e)** Gene expression ($-\Delta C_T$) of *Tnf*, *Cxcl1*, and *Socs3* in the cervix. **(f)** Representative images of cervical dilation and quantifications of cervical length and width. Scale bar represents 10 mm (n = 7–11 per group). **(g)** Heatmap representation of inflammatory gene expression in foetal membranes (n = 9 per group). Gene expression ($-\Delta C_T$) of **(h)** *Nlrp3*, *Nos2*, and *Mmp9* or **(i)** *Il1b*, *Ccl3*, *Ccr5*, and *Cxcl10* in foetal membranes. Data for gene expression are shown as box-and-whisker plots where midlines indicate medians, boxes indicate interquartile ranges, and whiskers indicate minimum and maximum values. p-values were determined by two-sided Mann–Whitney U-test. *p < 0.05; **p < 0.01; ***p < 0.001.

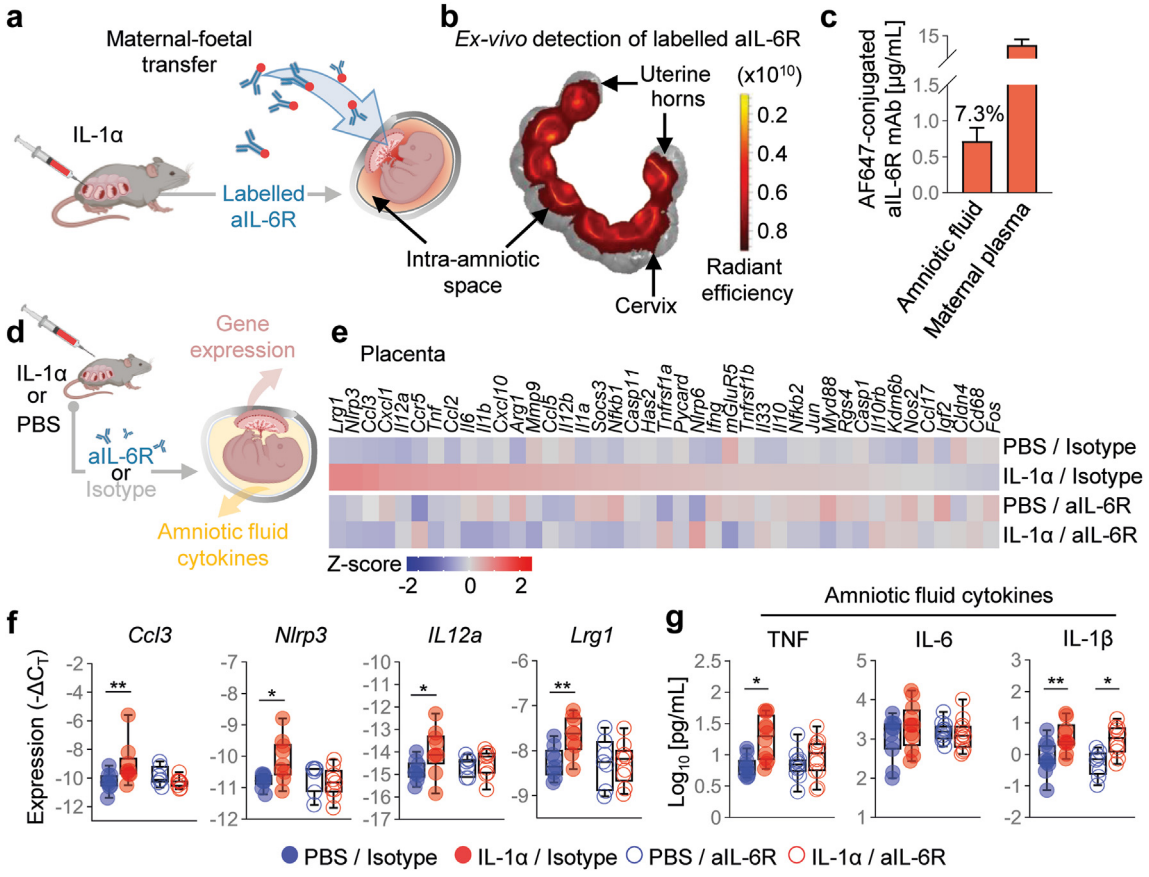

Fig. 4: **Anti-IL-6R efficiently crosses the placenta and reduces the inflammation-related gene expression induced by intra-amniotic IL-1α.** **(a)** Dams underwent intra-amniotic injection of IL-1α on 16.5 days *post coitum* (dpc). Six h later, dams received Alexa Fluor™647-conjugated rat anti-mouse IL-6 receptor monoclonal antibody (aIL-6R) to evaluate maternal–foetal transfer. Sixteen h after intra-amniotic injection the uterus was collected for imaging by using the IVIS system. **(b)** Representative fluorescence image and scale showing the *ex vivo* detection of labelled aIL-6R in the intra-amniotic space. **(c)** Amniotic fluid concentrations (µg/mL) of aIL-6R in the amniotic fluid and maternal plasma. The amniotic fluid concentration is also reported as a percentage of the maternal plasma concentration (7.3%) (n = 5). Data are shown as bar plots with mean and S.E.M. **(d)** Dams underwent intra-amniotic injection of PBS (control) or IL-1α on 16.5 days *post coitum* (dpc). Six h later, dams were treated with aIL-6R or rat IgG2b isotype (control). Sixteen h after intra-amniotic injection, placental tissues and amniotic fluid were collected to determine gene expression and cytokine concentrations, respectively. **(e)** Representative heatmap showing Z-scores (red and blue indicates increased and decreased expression, respectively) for gene expression across the placental tissues from the four experimental groups (n = 7–9 per group). **(f)** Expression ($-\Delta C_T$) of *Ccl3*, *Nlrp3*, *Il12a*, and *Lrg1* in the placental tissues from the four experimental groups. **(g)** Concentrations (pg/mL) of TNF, IL-6, and IL-1β in the amniotic fluid from the four experimental groups (n = 8–12 per group). Data for gene expression are shown as box-and-whisker plots where midlines indicate medians, boxes indicate interquartile ranges, and whiskers indicate minimum and maximum values. p-values were determined using the two-sided Mann–Whitney U-test. *p < 0.05; **p < 0.01.

foetal membrane/decidual activation, all of which involve a rise in pro-inflammatory mediators.[72–75] Thus, using an RT-PCR array, we measured the expression of several transcripts associated with inflammation in the uterus, cervix, foetal membranes, and decidua (Fig. 3a). Overall, the inflammatory signatures triggered by IL-1α-induced labour in each compartment were unique. For example, IL-1α-induced labour caused increased uterine expression of *Il1b, Nlrp3, Ccl2, Ccl5, Mmp9,* and *Nos2*; however, such overexpression was not observed upon treatment with aIL-6R (Fig. 3b and c). In the cervix, IL-1α-induced labour drove the increased expression of *Tnf, Cxcl1,* and *Socs3*, and these transcripts were reduced to control levels upon treatment with aIL-6R (Fig. 3d and e). Indeed, the process of cervical ripening was evident in dams injected with IL-1α but not in those treated with aIL-6R (Fig. 3f). In the foetal membranes, IL-1α-induced labour was associated with increased expression of *Nlrp3, Nos2,* and *Mmp9*, and such overexpression was dampened by aIL-6R treatment (Fig. 3g and h). However, IL-1α also induced the expression of *Il1b, Ccl3, Ccr5,* and *Cxcl10*, none of which were reduced upon treatment with aIL-6R (Fig. 3i). Furthermore, neither IL-1α-induced labour nor

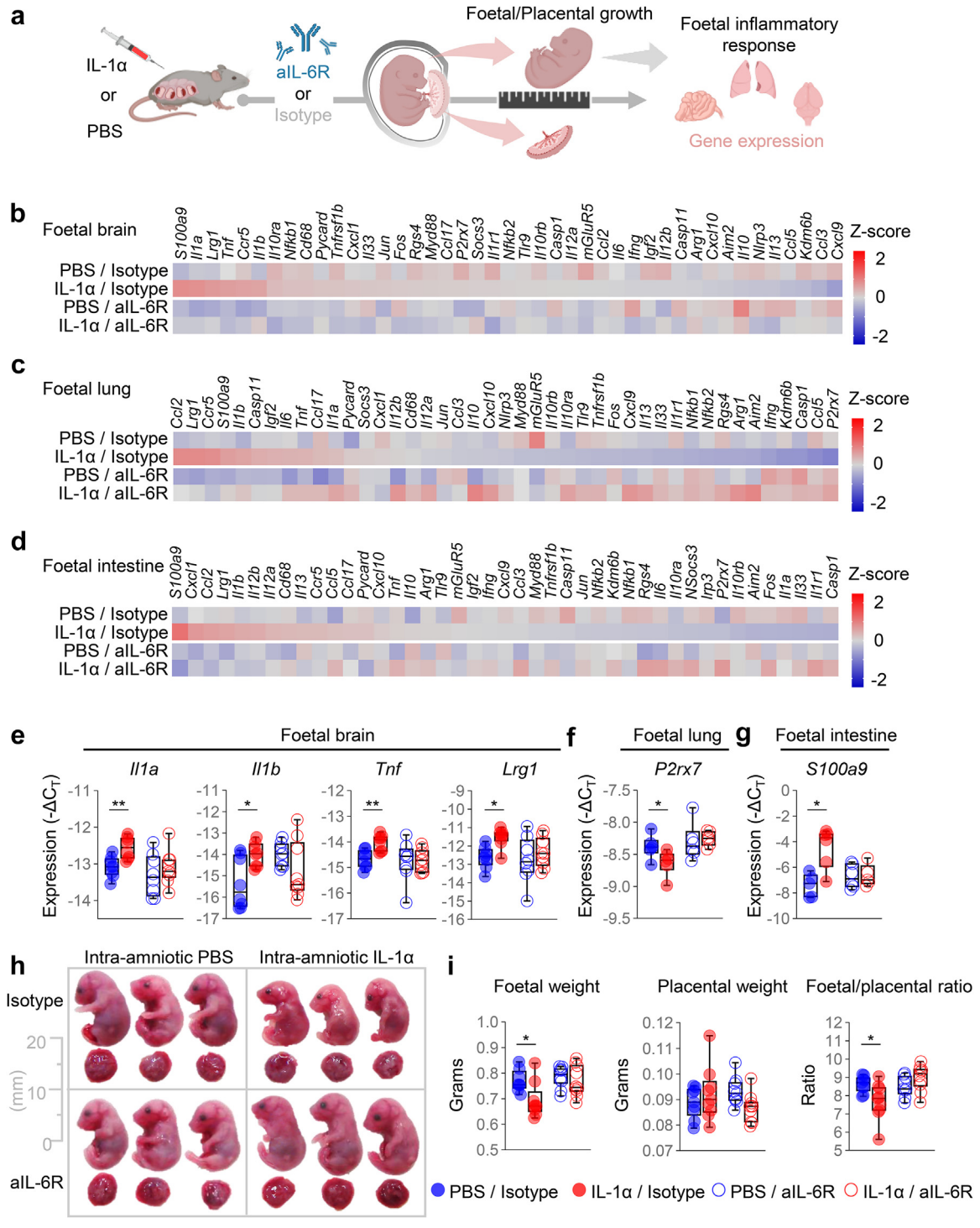

Fig. 5: **Anti-IL-6R dampens foetal inflammation induced by intra-amniotic IL-1α, restoring foetal growth**. **(a)** Dams underwent intra-amniotic injection of PBS (control) or IL-1α on 16.5 days *post coitum* (dpc). Six h later, dams received intraperitoneal injection of rat anti-mouse IL-6 receptor monoclonal antibody (aIL-6R) or rat IgG2b isotype (control). Sixteen h after intra-amniotic injection, foetal and placental growth parameters were measured followed by tissue collection to determine gene expression. Representative heatmaps showing Z-scores for gene expression in the **(b)** foetal brain, **(c)** foetal lung, and **(d)** foetal intestine from the four experimental groups (n = 6–9 per group). Red indicates increased expression and blue indicates decreased expression. Expression ($-\Delta C_T$) of **(e)** *Il1a*, *Il1b*, *Tnf*, and *Lrg1* in the foetal brain, **(f)** *P2rx7* in the foetal lung, and **(g)** *S100a9* in the foetal intestine from the four experimental groups. **(h)** Representative images of

treatment with aIL-6R modified the expression of decidual transcripts associated with an inflammatory response (Fig. S1). Taken together, these results indicate that IL-1α triggers the common pathway of labour in the uterus, cervix, and foetal membranes, inducing preterm birth in mice; yet, treatment with aIL-6R partly dampens these processes. The latter findings provide a mechanism whereby the blockade of IL-6R prevents premature labour.

aIL-6R crosses the maternal–foetal interface, restores foetal growth, and dampens foetal inflammation

The common pathway of labour is governed by maternal and foetal signalling, including within the intra-amniotic space.[56,76] Therefore, we next investigated whether aIL-6R administered systemically to dams can reach the intra-amniotic space and be detected in amniotic fluid (Fig. 4a). Using an Alexa Fluor™647-conjugated aIL-6R and imaging techniques, we showed that this antibody could be detected in the intra-amniotic space (Fig. 4b) and quantified in amniotic fluid (Fig. 4c), demonstrating maternal–foetal transfer.

Next, we investigated the effects of aIL-6R on the inflammatory response induced by IL-1α in the placenta and amniotic fluid (Fig. 4d). Treatment with aIL-6R prevented the IL-1α-induced expression of *Ccl3, Nlrp3, Il12a,* and *Lrg1* in the placenta (Fig. 4e and f). Furthermore, treatment with aIL-6R modulated the inflammatory response in the amniotic cavity, as evidenced by dampening of pro-inflammatory cytokines such as TNF and IL-6 (Fig. 4g). Treatment with aIL-6R tended to reduce the amniotic fluid concentration of IL-1β (Fig. 4g); yet, the bioactive form of this cytokine was not determined in this study.

We then evaluated whether treatment with aIL-6R could similarly ameliorate the foetal inflammatory response induced by IL-1α (Fig. 5a). Treatment with aIL-6R reduced the expression of specific mediators in the foetal brain, foetal lung, and foetal intestine, indicating that this antibody targets specific pathways in each compartment (Fig. 5b–d). For example, aIL-6R treatment prevented the IL-1α-driven dysregulation of *Il1a, Il1b, Tnf,* and *Lrg1* in the foetal brain (Fig. 5e), *P2rx7* in the foetal lung (Fig. 5f), and *S100a9* in the foetal intestine (Fig. 5g).

Intra-amniotic and foetal inflammation have been strongly associated with foetal growth restriction.[77–80] Therefore, we last investigated whether treatment with aIL-6R could have beneficial effects on foetal and placental growth (Fig. 5h). Treatment with aIL-6R protected against IL-1α-induced foetal growth restriction, as evidenced by the foetal:placental weight ratio (Fig. 5i).

Collectively, these data indicate that treatment with aIL-6R dampens the IL-1α-induced inflammatory response in the amniotic cavity containing the placenta, amniotic fluid, and foetus, thereby preventing foetal growth restriction, and that this protective effect is attained through the capacity of the treatment to reach the intra-amniotic space.

Blockade of IL-6R improves adverse neonatal outcomes induced by intra-amniotic IL-1α

Having established the protective effects of aIL-6R on the foetus, we next explored whether such benefits extended into neonatal life (Fig. 6a). Neonatal survival was negatively impacted by intra-amniotic exposure to IL-1α across the first three weeks of life; yet, such an adverse neonatal outcome was ameliorated by the blockade of IL-6R (Fig. 6b). The protective effect of aIL-6R on neonatal growth was also demonstrated by increased neonatal weight and size in the first three weeks of life (Fig. 6c and d). Intra-amniotic IL-1α had notable effects on neonatal head size; therefore, we also evaluated the biparietal diameter as a readout of brain mass and showed that the blockade of IL-6R prevented such an adverse neonatal outcome (Fig. 6e). To complement these observations, we performed neuromotor tests[62] in neonates exposed to intra-amniotic IL-1α and those treated with aIL-6R. Negative geotaxis is one of the earliest innate reflexes that neonates display after birth.[62,81] Neonates exposed to IL-1α *in utero* failed the negative geotaxis test more often and took longer to complete the test than control neonates, but such worsened performance was improved upon treatment with aIL-6R (Fig. 6f). Neonates exposed to IL-1α *in utero* also tended to fail the surface righting and cliff aversion tests; however, these alterations did not reach statistical significance (Fig. S2a and b). Nonetheless, treatment with aIL-6R did not affect test performance (Fig. S2a and b). Next, we evaluated brain inflammation in neonates exposed to IL-1α *in utero* and those treated with aIL-6R. Consistent with compromised neuromotor skills, the brain of neonates exposed to intra-amniotic IL-1α displayed upregulation of inflammatory mediators such as *Aim2, Cd68, Ccr5,* and *mGluR5*; yet, such overexpression was not observed after treatment with aIL-6R (Fig. 6g and h), suggesting that brain inflammation is dampened by the blockade of IL-6R. Last, we determined neonatal lung inflammation, given that premature neonates are at increased risk of pulmonary

foetuses and placentas from the four experimental groups. Scale bar represents 20 mm. **(i)** Foetal weight, placental weight, and foetal:placental weight ratio from the four experimental groups (n = 9–10 litters per group). Data for gene expression are shown as box-and-whisker plots where midlines indicate medians, boxes indicate interquartile ranges, and whiskers indicate minimum and maximum values. p-values were determined using the two-sided Mann–Whitney U-test. *p < 0.05; **p < 0.01.

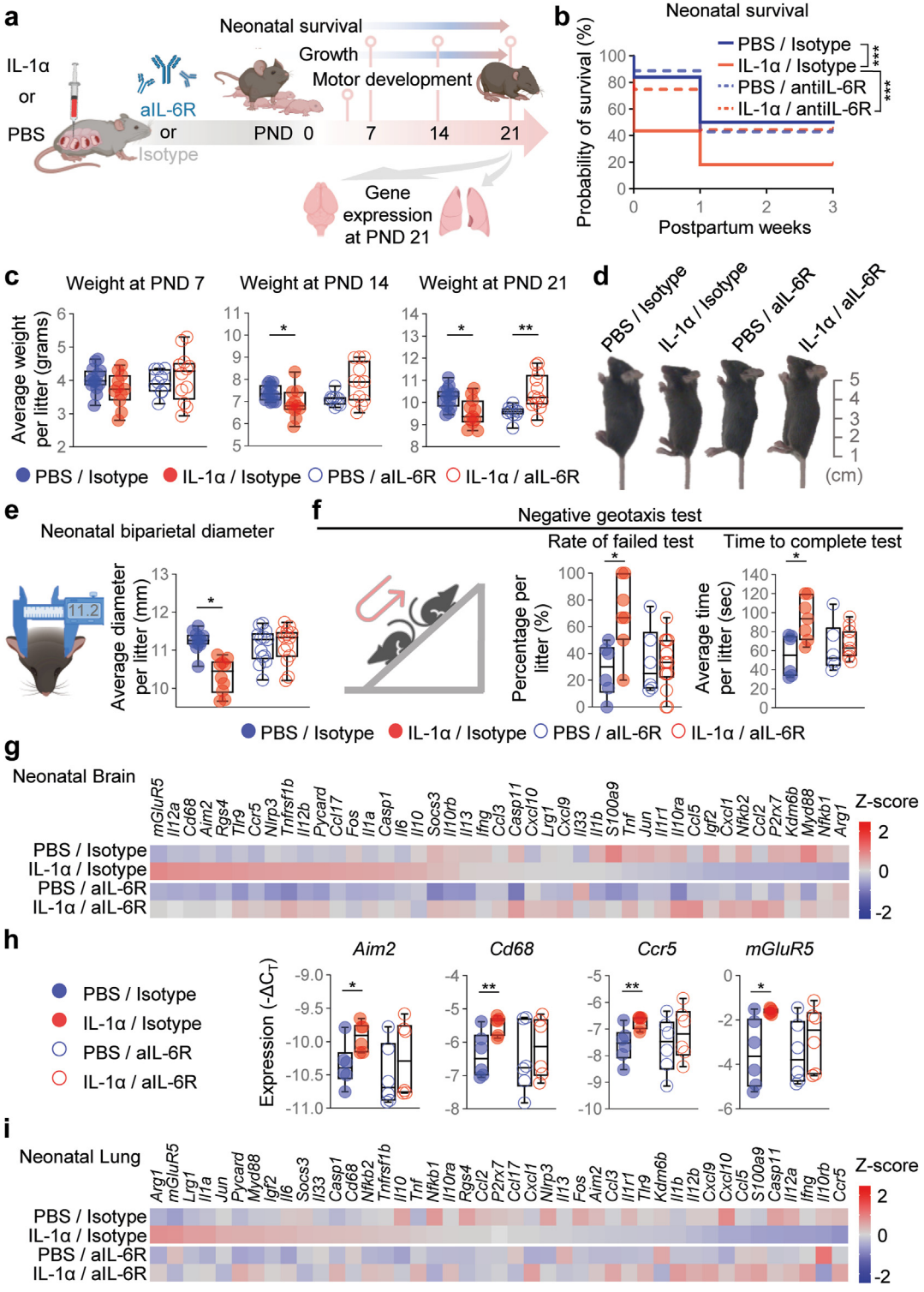

***Fig. 6:* Blockade of IL-6R improves neonatal outcomes and limits organ inflammation induced by intra-amniotic IL-1α. (a)** Dams underwent intra-amniotic injection of PBS (control) or IL-1α on 16.5 days *post coitum* (dpc). Six h later, dams received intraperitoneal injection of rat anti-mouse IL-6 receptor monoclonal antibody (aIL-6R) or rat IgG2b isotype (control). Dams were allowed to deliver and neonatal survival until postnatal day (PND) 21 as well as weekly weights and neuro-motor development testing were recorded. Brain and lung tissues were collected on PND21. **(b)** Neonatal survival rates up to PND21 are displayed as Kaplan–Meier survival curves (n = 14 litters per group). p-values

diseases such as respiratory distress syndrome or bronchopulmonary dysplasia, among others.[82,83] Neonates exposed to IL-1α *in utero* did not display a strong dysregulation of the targeted inflammatory markers in their lungs (Fig. 6i), suggesting that the inflammatory milieu in SIAI is milder than that associated with bacteria, which is associated with severe neonatal respiratory diseases.[84–86] Taken together, these findings highlight the deleterious effects of elevated IL-1α *in utero* and provide strong evidence that the blockade of IL-6R enhances neuromotor skills, dampens brain inflammatory responses, and improves neonatal growth, protecting against adverse perinatal outcomes.

Blockade of IL-6R restores IL-1α-induced neonatal gut immune-microbiome alterations

Premature human neonates display alterations of the gut microbiome.[87,88] Indeed, maternal systemic inflammation, largely driven by IL-6, leads to neonatal gut dysbiosis.[89] Moreover, preterm neonates born to patients with chorioamnionitis are at higher risk of necrotizing enterocolitis[90,91]; yet, whether sterile intra-amniotic inflammation, the most common inflammatory response *in utero*,[20] causes neonatal gut inflammation or alteration of the gut microbiome is unknown. To address this, we first evaluated inflammatory gene expression in the murine neonatal gut, which was divided into the small intestine, caecum, and colon (Fig. 7a). Intra-amniotic IL-1α altered the gene expression profile of each intestinal compartment, an effect that was partially reversed by prenatal treatment with aIL-6R (Fig. 7b–d). Specifically, treatment with aIL-6R fostered homeostasis by preventing the IL-1α-driven dysregulation of *Ccr5, Casp1* and *Il12b* in the small intestine (Fig. 7e), *Socs3, Ccr5* and *Casp1* in the caecum (Fig. 7f), and *Aim2, Myd88, Ccl17, Ccr5, Ifng* and *Il12a* in the colon (Fig. 7g).

To characterise the neonatal gut microbiome, we performed metagenomic (i.e., shotgun) sequencing of the neonatal small intestine, caecum, and colon (Fig. S3a). Overall, the distribution of major microbial phyla remained consistent among study groups for each tissue, as did the *Bacillota:Bacteroidota* ratio that is reflective of normal intestinal homeostasis (Fig. S3b). Alpha diversity metrics of the microbiome indicated that IL-1α was associated with altered community evenness in the colon, which was not observed in aIL-6R-treated mice (Fig. S3c). We then analysed beta diversity of the microbiome in each segment of the neonatal gut (Fig. 8a–l and Fig. S4). IL-1α exposure was associated with changes in community structure in the caecum (Fig. 8a–c) and the colon (Fig. 8g–i), but not in the small intestine (Fig. S3d). In the caecum and colon, several bacterial taxa showed altered abundance (Fig. S4a and b). Importantly, aIL-6R treatment prevented the IL-1α-driven microbiome alterations in the caecum (Fig. 8d–f and Fig. S4a) and colon (Fig. 8j–l and Fig. S4b) as evidenced by the lack of differences in microbial community structure and individual taxa abundance between treatment and control groups.

Intra-amniotic administration of IL-1α induced immune dysregulation in the neonatal gut (Fig. S5a). Yet, treatment with aIL-6R mainly restored the neonatal microbiome in the caecum and colon; therefore, we focused on evaluating cellular immune responses in these compartments using immunophenotyping in two groups: neonates born to dams that were injected with IL-1α and those treated with aIL-6R (Fig. 9a). We first evaluated general leukocyte populations including total leukocytes ($CD45^+$ cells), myeloid cells ($CD11b^+$ cells), conventional T cells ($CD3^+$ cells), mucosal-associated invariant T (MAIT) cells ($TCRVb6^+$ cells), NK cells ($ID2^+NK1.1^+$ cells), and innate lymphoid cells (ILCs) ($ID2^+$ cells) (Fig. S5b). The majority of affected leukocyte populations between study groups were conventional T and MAIT cells, ILCs, and NK cells (Fig. 9b). Then, we focused on specific subsets of these lymphoid cells identified by the expression of transcription factors or cytokines. Overall, treatment with aIL-6R restored cellular immune homeostasis. Specifically, in the neonatal caecum, treatment with aIL-6R reduced the IL-1α-driven increase in the proportions of $CD4^+ROR\gamma t^+$ T cells, $CD8^+Foxp3^+$ T cells, $CD8^+IL\text{-}17A^+$ T cells, $CD4^+Foxp3^+$ MAIT cells, $CD8^+IL\text{-}17A^+$ MAIT cells,

were determined using the Gehan-Breslow-Wilcoxon test. **(c)** Weights (g) of neonates across the first three weeks of life are shown as box plots (n = 10–14 litters per group). p-values were determined using two-sided Mann–Whitney U-tests. Data are shown as box-and-whisker plots where midlines indicate medians, boxes indicate interquartile ranges, and whiskers indicate minimum and maximum values. **(d)** Representative images of pups at PND21. The scale bar represents 5 cm. **(e)** Schematic diagram of calliper measurement and quantification of neonatal biparietal diameter (n = 10–14 litters per group). **(f)** Schematic diagram of the negative geotaxis test for neuro-motor evaluation. The rate of neonates with a failed test and the time required to complete the test are shown as box plots (n = 6–14 litters per group). Data in e and f are shown as box-and-whisker plots where midlines indicate medians, boxes indicate interquartile ranges, and whiskers indicate minimum and maximum values. **(g)** Representative heatmap showing Z-scores for gene expression in the neonatal brain from the four experimental groups (n = 6 per group). Red indicates increased expression and blue indicates decreased expression. **(h)** Expression ($-\Delta C_T$) of *Aim2, Cd68, Ccr5*, and *mGluR5* in the neonatal brain. Data for gene expression are shown as box-and-whisker plots where midlines indicate medians, boxes indicate interquartile ranges, and whiskers indicate minimum and maximum values. **(i)** Representative heatmap showing Z-scores for gene expression in the neonatal lung from the four experimental groups (n = 6 per group). p-values were determined using the two-sided Mann–Whitney U-test. *p < 0.05; **p < 0.01.

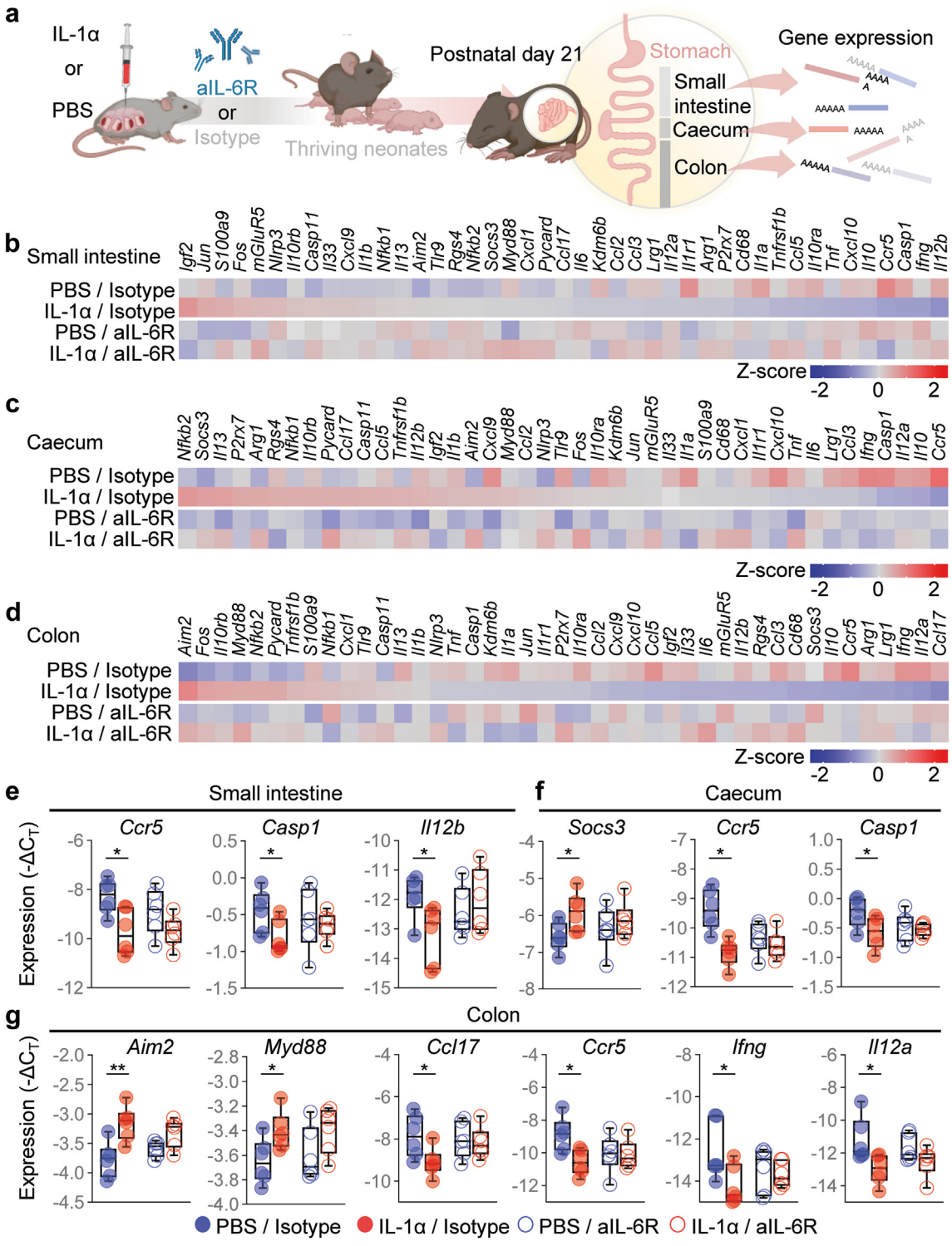

***Fig. 7*: Blockade of IL-6R prevents IL-1α-induced neonatal gut inflammation.** **(a)** Dams underwent intra-amniotic injection of PBS (control) or IL-1α on 16.5 days post coitum (dpc). Six h later, dams received intraperitoneal injection of rat anti-mouse IL-6 receptor monoclonal antibody (aIL-6R) or rat IgG2b isotype (control). Dams were allowed to deliver, and the neonatal small intestine, caecum, and colon were collected on postnatal day (PDN) 21 to determine gene expression. Representative heatmaps showing Z-scores for gene expression in the neonatal **(b)** small intestine, **(c)** caecum, and **(d)** colon from the four experimental groups (n = 6 per group). Red indicates increased expression

$CD8^+GATA3^+$ MAIT cells, $TGF\beta^+$ ILCs, $NCR^+TGF\beta^+$ ILCs, $ROR\gamma t^+$ NK cells, and $IFN\gamma^+$ NK cells (Fig. 9c). In the colon, treatment with aIL-6R dampened the proportions of $CD4^+ROR\gamma t^+$ T cells, $CD8^+IL\text{-}17A^+$ T cells, $CD4^+Foxp3^+$ MAIT cells, $NCR^+TGF\beta^+$ ILCs, $NCR^+IL\text{-}10^+$ ILCs, and $IFN\gamma^+$ NK cells observed upon IL-1α exposure (Fig. 9d).

Collectively, these findings indicate that treatment with aIL-6R not only prevents PTB induced by SIAI but, more importantly, improves adverse neonatal outcomes by restoring gut immune-microbiome homeostasis.

Discussion

The study herein provides a mechanistic investigation supporting the hypothesis that the use of a monoclonal antibody against IL-6R is a potential therapy for preventing PTB and adverse neonatal outcomes induced by SIAI, thereby representing a feasible intervention for this clinical condition that has no currently approved treatment. The treatment of pathologies involving sterile inflammation in non-pregnant individuals include non-steroidal anti-inflammatory drugs[92] or other specific therapies[93,94] that are not clinically approved to be used during pregnancy due to their potentially harmful effects on the foetus.[95,96] Therefore, the urgent need to find safe treatments for SIAI has led us to pursue a strategy for repurposing drugs with anti-inflammatory properties that are already safely utilised during pregnancy. Previously, we demonstrated that betamethasone, a corticosteroid that has been shown to accelerate foetal organ maturation in patients at risk of delivering preterm,[97,98] prevented alarmin-induced PTB but not the consequent neonatal mortality.[58] Then, we showed that clarithromycin, a macrolide that in combination with other antibiotics can be used to treat microbial intra-amniotic inflammation,[99–102] prevented alarmin-induced PTB and neonatal mortality by interfering with the common pathway of labour as well as by reducing the inflammatory responses in foetal organs.[59] Yet, the effects of such drugs on neonatal neurodevelopment and gut host-immune responses have not been evaluated. The recent COVID-19 pandemic represented a challenge for science, given that effective preventive strategies as well as treatments to avoid worsening of the disease need to be applied in a timely fashion. The field of obstetrics was even more challenged, since the effects of COVID-19 itself, as well as the safety of the proposed treatments, must be evaluated for two individuals (i.e., the mother and the foetus). In this regard, case reports from the beginning of the pandemic described the use of the IL-6R mAb, tocilizumab, as a treatment for severe COVID-19 in pregnant individuals.[36,37,103] Months later, cases of pregnant patients treated with tocilizumab had increased, showing maternal benefits without deleterious effects on the foetus.[39,40,104–108] Anti-IL-6R has traditionally been a safe option to treat pregnant individuals with autoimmune diseases such as rheumatoid arthritis.[34,109,110] Moreover, previous reports have demonstrated that either the absence of the *Il6* gene ($Il6^{-/-}$ mouse model),[31] pre-treatment with a rat anti-mouse IL-6R antibody (MR16-1),[42] or co-treatment with an anti-IL-6 antibody[43] in dams receiving systemic administration of LPS reduced the rate of PTB.[42] However, the use of drugs for pre-treatment of prematurity has limited translational value given that pregnant individuals are unlikely to accept prophylactic treatment in the absence of symptoms. Moreover, the administration of drugs prior to diagnosis (i.e., prophylaxis) is not suitable for sterile intra-amniotic inflammation since there is currently no reliable predictive model to identify patients who will develop this obstetrical disease. Furthermore, the intra-peritoneal injection of LPS is a model of endotoxemia, which may resemble the clinical conditions of clinical chorioamnionitis or pyelonephritis during pregnancy[53,111]; yet, such obstetrical diseases can be successfully treated with antibiotics.[112–114] Our results demonstrating that aIL-6R can prevent PTB and adverse neonatal outcomes exclusively in the context of SIAI, but not in microbial intra-amniotic inflammation, are in line with a previous report showing no differences in the rate of PTB in $Il6^{-/-}$ dams receiving intra-uterine injection of *E. coli* compared to controls.[115] Together with these investigations, our findings demonstrate the differential effects of local and systemic inflammation as well as their sterile or microbe-associated nature during pregnancy, highlight the distinct features of these entities, and reinforce the fact that targeted therapeutic approaches are required to prevent prematurity in distinct subsets of pregnant patients.

Herein, we demonstrated that one mechanism whereby aIL-6R prevents PTB is by dampening the IL-1α-induced inflammatory response in reproductive and gestational tissues that participate in the common pathway of parturition, namely the uterus, foetal membranes/decidua, and cervix.[10,72–75] It is well known that the components of the IL-6 pathway are widely expressed in the reproductive and gestational tissues,[116] and IL-6 signalling is involved in key physiologic reproductive events such as implantation and labour.[31,32,116] In the context of SIAI, alarmins were shown to induce an inflammatory milieu in the tissues

and blue indicates decreased expression. Expression (−ΔCT) of **(e)** *Ccr5*, *Casp1*, and *Il12b* in the neonatal small intestine, **(f)** *Socs3*, *Ccr5*, and *Casp1* in the neonatal caecum, and **(g)** *Aim2*, *Myd88*, *Ccl17*, *Ccr5*, *Ifng*, and *Il12a* in the neonatal colon from the four experimental groups. Data for gene expression are shown as box-and-whisker plots where midlines indicate medians, boxes indicate interquartile ranges, and whiskers indicate minimum and maximum values. p-values were determined using the two-sided Mann–Whitney U-test. *$p < 0.05$; **$p < 0.01$.

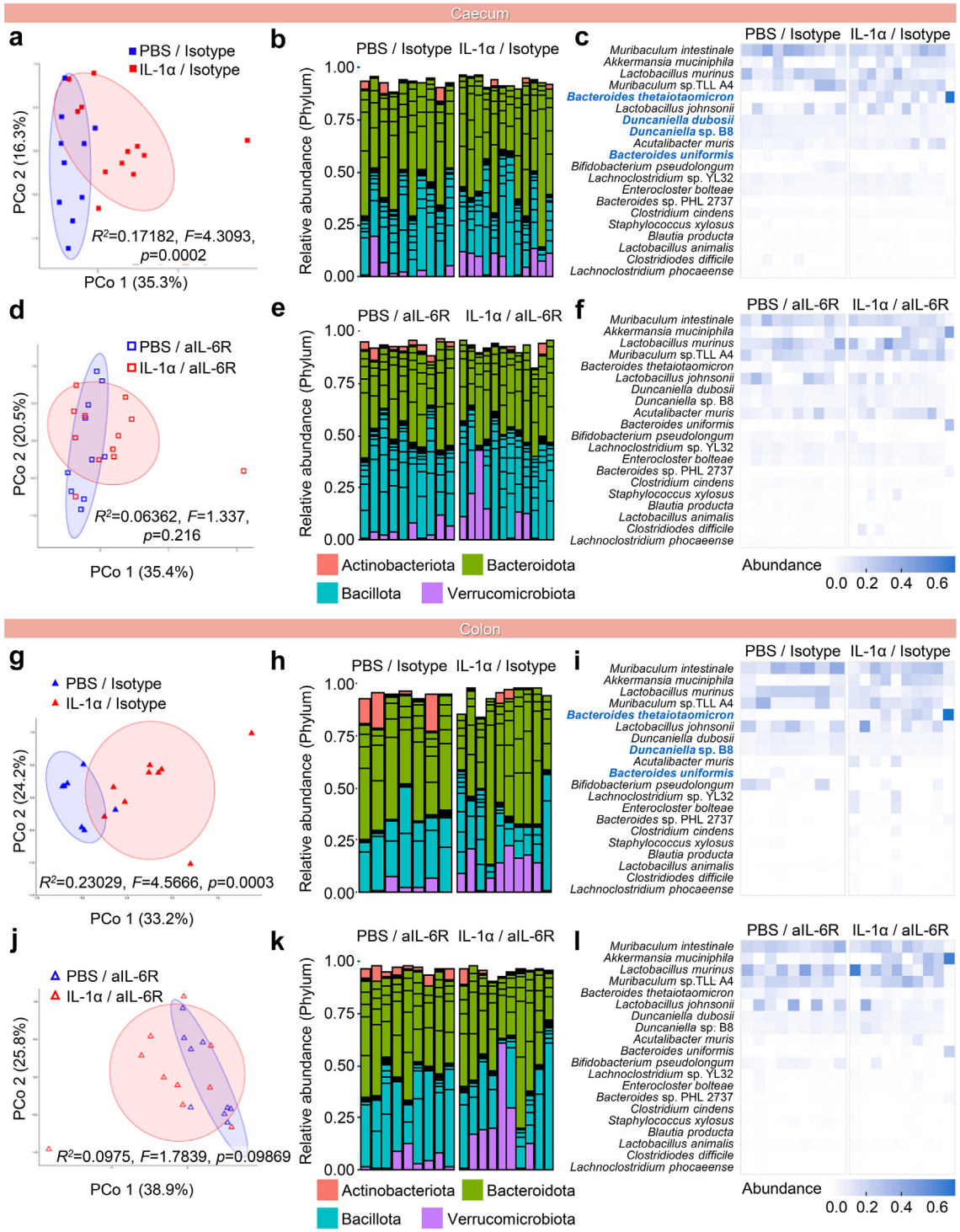

Fig. 8: **Blockade of IL-6R prevents IL-1α-induced microbiome alterations in the neonatal caecum and colon**. Samples from the neonatal colon and caecum, as well as environmental controls, were obtained at postnatal day 21 using sterile swabs. **(a–f)** Principal coordinate analysis (PCoA) illustrating variation in the metagenomic profiles of the neonatal caecum of the **(a)** PBS/Isotype and IL-1α/Isotype groups or **(d)** PBS/aIL-6R and IL-1α/aIL-6R groups (n = 10–12 per group). Bar plots showing the taxonomic classifications of the 20 bacterial taxa with highest relative abundance in the neonatal caecum of the **(b)** PBS/Isotype and IL-1α/Isotype groups or **(e)** PBS/aIL-6R and IL-1α/aIL-6R groups (n = 10–12 per group). Heatmap displaying the relative abundance and taxonomy of the 20 most relatively abundant bacterial taxa between the

included in the common pathway of labour in humans[117–123] and mice.[30,124] Notably, a previous investigation demonstrated that tocilizumab reduced the IL-6-induced expression of metalloproteinase-9 in amnion epithelial cells,[125] which is in line with our results in foetal membranes. Moreover, tocilizumab dampens the myometrial cell proliferation induced by leptin,[126] a protein that has been implicated in the onset of labour.[127,128] To our knowledge, no previous research had evaluated the effects of aIL-6R in cervical ripening. Regardless of the scarcity of research on the effects of aIL-6R in gestational tissues, a recent human case report demonstrated that tocilizumab can cross the placenta, as evidenced by a high concentration of the drug in the cord blood.[129] Yet, the concentration of aIL-6R in the amniotic fluid had not been previously evaluated. Therefore, our results showing that aIL-6R reaches the amniotic fluid and dampens the intra-amniotic inflammatory response induced by alarmins represent a previously unknown mechanism whereby aIL-6R can prevent PTB and adverse foetal and neonatal outcomes.

Foetal exposure to intra-amniotic inflammation or intra-amniotic infection has been linked to restricted foetal growth, neuroinflammation, and impaired neurodevelopment[77–80,130–133] that, in turn, is associated with a number of adverse neurologic outcomes and mental diseases.[132,134,135] Reports linking foetal inflammation to adverse neurodevelopmental outcomes were primarily focused on intra-amniotic infection rather than SIAI; yet, studies investigating the resulting foetal inflammatory response have indicated that inflammatory mediators are the driving factor in the resulting foetal damage, regardless of the microbial or sterile nature of the initial insult.[130,136,137] Indeed, the potential mechanisms whereby inflammatory cytokines can induce foetal neurological damage include direct effects on cerebral vasculature resulting in hypoperfusion and ischemia, activation of the coagulation cascade causing thrombosis and necrosis, microglial activation leading to propagation of the inflammatory response, and increased blood–brain barrier permeability.[130] The above data therefore suggest that the targeting of key inflammatory mediators or their signalling pathways could represent a viable approach to prevent the neonatal consequences of *in utero* inflammation exposure, including neurological damage leading to adverse neurodevelopmental outcomes. Consistent with this concept, herein we report that prenatal neutralisation of IL-6R prevented neonatal growth impairment, including a diminished biparietal diameter, and improved neonatal performance in behavioural tests designed to evaluate neurodevelopment.[62] Such improved observational outcomes were associated with reduced inflammatory gene expression in the neonatal brain, allowing us to propose a mechanism whereby IL-6R blockade prevents inflammatory signalling in this organ, restoring the normal trajectory of neonatal growth and neurodevelopment.

In line with our findings in the neonatal brain, the blockade of IL-6R signalling was found to ameliorate the neonatal gut inflammation driven by *in utero* exposure to IL-1α. Such dampening of the immune response included altered intestinal gene expression and the reduced presence of specific leukocyte subsets. Our model of alarmin-induced intra-amniotic inflammation is consistent with a prior study in which the intra-amniotic administration of IL-1α to pregnant sheep resulted in upregulation of inflammatory gene expression in the foetal ileum together with increased T cells and myeloperoxidase $(MPO)^+$ cells.[138] The detrimental effects of inflammatory insults on the foetal gut were further demonstrated by direct exposure of the ovine foetal intestine to LPS, resulting in similar tissue inflammation and leukocyte infiltration.[139] Furthermore, selective *in utero* exposure of the ovine foetal gut to IL-1α also caused local inflammation and leukocyte infiltration.[140] Finally, preterm piglets exposed to intra-amniotic LPS displayed signs of gut inflammation at birth and prolonged systemic inflammation at postnatal day 5,[141] further supporting the prolonged adverse effects of *in utero* exposure to an inflammatory insult. Indeed, the exposure of murine foetuses to maternal systemic inflammation induced by intraperitoneal LPS was also found to cause intestinal inflammation and impaired development in neonatal life.[142] Moreover, such a response was at least partially IL-6-dependent, as mice deficient for this cytokine displayed reduced signs of neonatal inflammation.[142] Together with data presented herein, these studies support the role of the IL-6 signalling pathway in foetal and neonatal gut inflammation

metagenomic profiles of the neonatal caecum of the **(c)** PBS/Isotype and IL-1α/Isotype groups or **(f)** PBS/aIL-6R and IL-1α/aIL-6R groups (n = 10–12 per group). **(g–l)** PCoA illustrating variation in the metagenomic profiles of the neonatal colon of the **(g)** PBS/Isotype and IL-1α/Isotype groups or **(j)** PBS/aIL-6R and IL-1α/aIL-6R groups (n = 10–12 per group). Bar plots showing the taxonomic classifications of the 20 bacterial taxa with highest relative abundance in the neonatal colon of the **(h)** PBS/Isotype and IL-1α groups/Isotype or **(k)** PBS/aIL-6R and IL-1α/aIL-6R groups (n = 10–12 per group). Heatmap displaying the relative abundance and taxonomy of the 20 most relatively abundant bacterial taxa between the metagenomic profiles of the neonatal colon of the **(i)** PBS/Isotype and IL-1α/Isotype groups or **(l)** PBS/aIL-6R and IL-1α/aIL-6R groups (n = 10–12 per group). Similarities in the metagenomic profiles (PCoA plots) were characterised using the Bray–Curtis similarity index. For bar plots, multiple taxa with the same phylum-level classification within the same sample are indicated by bars of the same colour. For heatmaps, bacterial taxa with significantly altered abundance between groups are labelled in blue. p-values were determined using two-sided Mann–Whitney U-tests with Holm's correction for multiple comparisons.

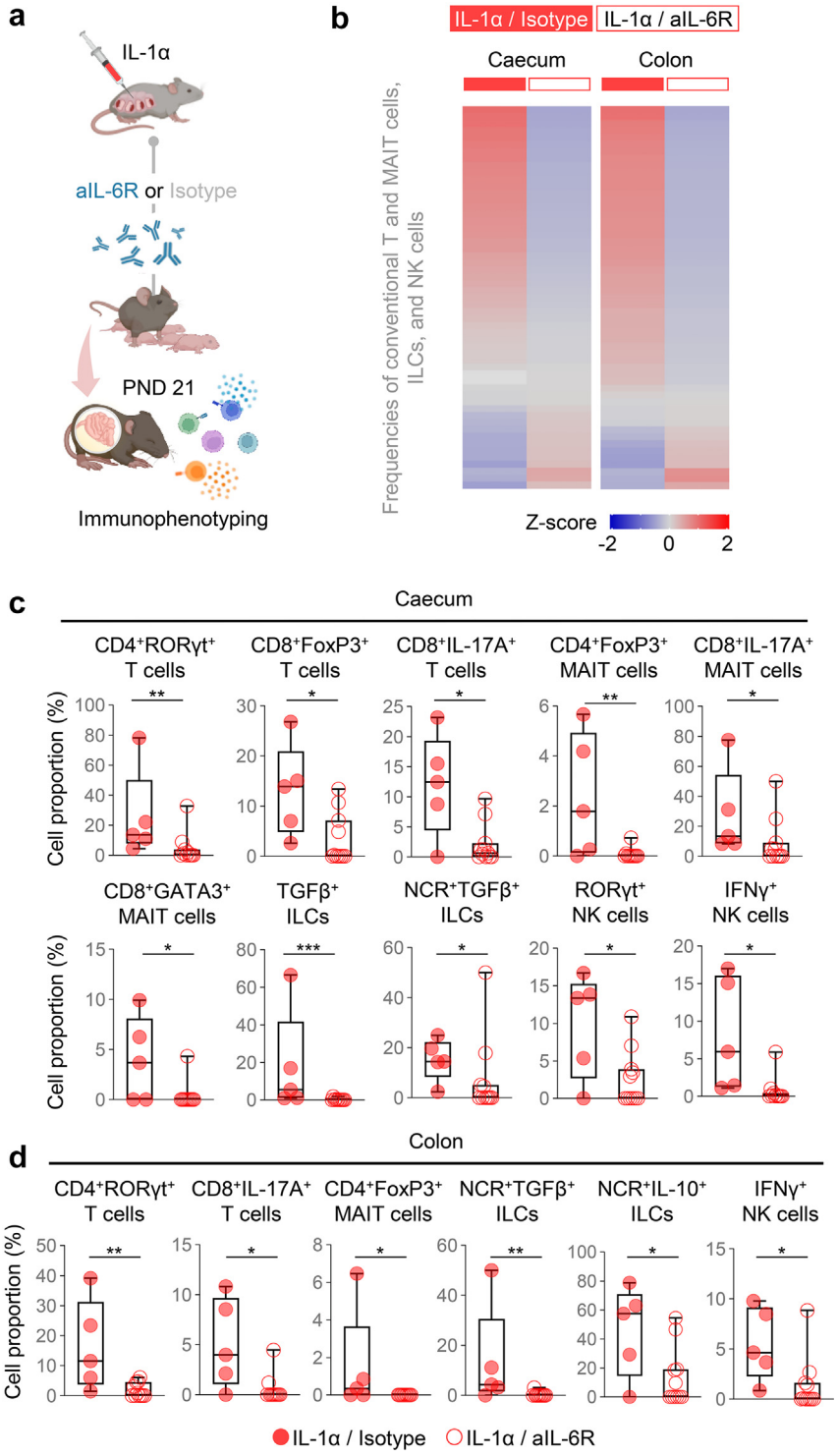

***Fig. 9:* Blockade of IL-6R restores immune cellular homeostasis in the neonatal gut following intra-amniotic IL-1α exposure.** **(a)** Dams underwent intra-amniotic injection of IL-1α on 16.5 days *post coitum* (dpc). Six h later, dams received intraperitoneal injection of rat anti-mouse IL-6 receptor monoclonal antibody (aIL-6R) or rat IgG2b isotype (control). Dams were allowed to deliver, and the neonatal small intestine, caecum, and colon were collected on postnatal day (PDN) 21 to isolate leukocytes for immunophenotyping. **(b)** Heatmap representation showing Z-scores for the proportions of specific lymphocyte subpopulations (conventional T and MAIT cells, ILCs, and NK cells) from the two experimental groups in the neonatal caecum and colon (n = 5–11 per group). **(c)** Cell proportions of $CD4^+ROR\gamma t^+$ T cells, $CD8^+FoxP3^+$ T cells,

resulting from exposure to intra-amniotic insults and provide further mechanistic support for the protective effects of aIL-6R observed in the current study.

The developmental period from late gestation through early neonatal life is critical for the formation of a healthy gut microbiome,[143] and multiple inflammatory, metabolic, neurologic, cardiovascular, and gastrointestinal diseases have been linked to disruption of the microbiota during this time.[144] Deep characterisation of the foetal gut using single-cell approaches has indicated that the formation of memory T cells in this compartment occurs in mid to late gestation,[145–147] likely driven by exposure to maternally derived antigens originating from microbes or other sources. Therefore, exposure to inflammation during this critical window of development is likely to hamper the proper establishment of the gut immunological niche, with subsequent consequences for the formation of the gut microbiome after delivery. Indeed, the presence of histologic lesions associated with intra-amniotic inflammation/infection (i.e., acute chorioamnionitis and funisitis) has been linked to alterations in the microbial composition of neonatal stool samples.[148] Moreover, studies have indicated that the risk of gut dysbiosis is increased in neonates born prematurely,[143] thus rapid treatment to minimise foetal exposure in cases of inflammation-associated preterm labour and birth is essential to prevent long-term alterations of the gut microbiota. Animals have been used to demonstrate the effects of direct treatment of neonates with gut dysbiosis using techniques such as faecal microbiota transplantation,[149] lactic acid-producing bacterial supplementation,[150] and pre/post-biotics,[143] among others. Yet, a potential advantage of maternal treatment with aIL-6R or other anti-inflammatory agents is that the initial inflammatory insult can be dampened, thereby reducing or completely avoiding foetal exposure that could result in neonatal gut dysbiosis and other adverse consequences. Nonetheless, additional research is required to evaluate the neonatal gut microbiome changes associated with SIAI and the role of IL-6R-mediated signalling in this process.

This study is not exempt from some limitations. Given that the main research question was to evaluate the use of aIL-6R as a treatment for SIAI induced by the intra-amniotic injection of IL -1α, our analysis did not address the roles of IL-6R signalling during normal pregnancy. However, we consider that administering aIL-6R as a prophylactic drug to pregnant individuals who are not at risk for PTB would be inadequate, thus we propose the use of aIL-6R as a treatment for a subset of patients with SIAI. Strengths of this study include the use of a model resembling the clinical scenario of SIAI, where the antibody treatment of a patient could be considered after the diagnosis of SIAI in the presence of an episode of preterm labour. The translational value of the proposed therapeutic strategy is based on a comprehensive and integrative approach that considered the potential benefits of this treatment not only during pregnancy but also in early neonatal life.

Collectively, the results presented herein demonstrate that the adverse perinatal outcomes triggered by the alarmin IL-1α can be prevented by the blockade of the IL-6R, underscoring the role of the IL-6 signalling pathway in the premature onset of labour associated with SIAI. Importantly, we demonstrate that such prenatal treatment prevents adverse long-term consequences of foetal exposure to intra-amniotic inflammation, including dampened inflammation in neonatal organs, improved neurodevelopment, restored immune cellular homeostasis of the neonatal gut, and reversal of gut microbiome dysbiosis, among others. Our results provide mechanistic evidence supporting the potential use of prenatal aIL-6R treatment as a therapeutic approach to not only prevent PTB resulting from SIAI but also to improve quality of life for the offspring.

Contributors

Conceptualisation: R.R., N.G.-L.
Methodology: M.F.-J., J.G., Y.X., B.A.B., B.P., N.G.-L.
Validation: M.F.-J., J.G., Y.X., V.G.-F., M.A.-H., N.G.-L.
Formal analysis: M.F.-J., J.G., Y.X., M.A.-H., A.D.W., B.A.B., R.H.P., R.P.-R., N.G.-L.
Investigation: M.F.-J., J.G., Y.X., D.M., V.G.-F., M.A.-H., B.A.B., Y.S., T.K., B.P., C.R.G., N.G.-L.
Resources: R.R., B.A.B., K.R.T., N.G.-L.
Data curation: M.F.-J., Y.X., V.G.-F., M.A.-H., A.D.W.
Writing—original draft: M.F.-J., J.G., D.M., N.G.-L.
Writing—review & editing: M.F.-J., J.G., Y.X., D.M., V.G.-F., M.A.-H., A.D.W., B.A.B., R.H.P., Y.S., T.K., B.P., C.R.G., R.P.-R., K.R.T., N.G.-L.
Visualisation: M.F.-J., J.G., V.G.-F., A.D.W., N.G.-L.
Supervision: R.R., B.A.B., K.R.T., N.G.-L.
Project administration: N.G.-L.
Funding acquisition: R.R., N.G.-L.
All authors read and approved the final version of the manuscript. M.F.-J., J.G., and N.G.-L. have accessed and verified all data underlying the findings presented in the manuscript. Each contributing author has accessed and verified the data that they were responsible for generating and/or analysing.

$CD8^+IL\text{-}17A^+$ T cells, $CD4^+FoxP3^+$ mucosal-associated invariant T (MAIT) cells, $CD8^+IL\text{-}17A^+$ MAIT cells, $CD8^+GATA3^+$ MAIT cells, $TGF\beta^+$ ILCs, $NCR^+TGF\beta^+$ ILCs, $ROR\gamma t^+$ NK cells, and $IFN\gamma^+$ NK cells in the neonatal caecum. **(d)** Cell proportions of $CD4^+ROR\gamma t^+$ T cells, $CD8^+IL\text{-}17A^+$ T cells, $CD4^+FoxP3^+$ MAIT cells, $NCR^+TGF\beta^+$ ILCs, $NCR^+IL\text{-}10^+$ ILCs, and $IFN\gamma^+$ NK cells in the neonatal colon. Data are shown as box-and-whisker plots where midlines indicate medians, boxes indicate interquartile ranges, and whiskers indicate minimum and maximum values. p-values were determined using the two-sided Mann–Whitney U-test. *$p < 0.05$; **$p < 0.01$; ***$p < 0.001$.

Data sharing statement

Single-cell RNA-sequencing data of the human chorioamniotic membranes were obtained from NCBI dbGaP phs001886.v1.p1 as originally reported in.[45] Single-cell RNA-sequencing data of the murine tissues were obtained from the Gene Expression Omnibus (GSE200289) as originally reported in.[52] Metagenomics files and associated metadata have been uploaded to the National Center for Biotechnology Information's Sequence Read Archive (PRJNA929530). All other data are presented within the current manuscript and/or its supplementary materials.

Declaration of interests

The authors declare no competing interests.

Acknowledgements

This research was supported by the Perinatology Research Branch (PRB), Division of Obstetrics and Maternal-Fetal Medicine, Division of Intramural Research, *Eunice Kennedy Shriver* National Institute of Child Health and Human Development, National Institutes of Health, U.S. Department of Health and Human Services (NICHD/NIH/DHHS) under Contract No. HHSN275201300006C. This research was also supported by the Wayne State University Perinatal Initiative in Maternal, Perinatal and Child Health. R.R. has contributed to this work as part of his official duties as an employee of the United States Federal Government. The authors gratefully acknowledge the members of the Biomarkers, Translational Science, and Microbiome Units of the PRB for their support with some molecular biology experiments. We also acknowledge Tzu Ning (Emily) Liu, a rotating medical student, who assisted with the set-up and validation of neurobehavioral tests in murine neonates.

Appendix A. Supplementary data

Supplementary data related to this article can be found at https://doi.org/10.1016/j.ebiom.2023.104865.

References

1 Liu L, Oza S, Hogan D, et al. Global, regional, and national causes of under-5 mortality in 2000-15: an updated systematic analysis with implications for the Sustainable Development Goals. *Lancet*. 2016;388(10063):3027–3035.
2 Chawanpaiboon S, Vogel JP, Moller AB, et al. Global, regional, and national estimates of levels of preterm birth in 2014: a systematic review and modelling analysis. *Lancet Glob Health*. 2019;7(1):e37–e46.
3 Perin J, Mulick A, Yeung D, et al. Global, regional, and national causes of under-5 mortality in 2000-19: an updated systematic analysis with implications for the Sustainable Development Goals. *Lancet Child Adolesc Health*. 2022;6(2):106–115.
4 Blencowe H, Lee AC, Cousens S, et al. Preterm birth-associated neurodevelopmental impairment estimates at regional and global levels for 2010. *Pediatr Res*. 2013;74 Suppl 1(Suppl 1):17–34.
5 Ream MA, Lehwald L. Neurologic consequences of preterm birth. *Curr Neurol Neurosci Rep*. 2018;18(8):48.
6 Jasper EA, Cho H, Breheny PJ, Bao W, Dagle JM, Ryckman KK. Perinatal determinants of growth trajectories in children born preterm. *PLoS One*. 2021;16(1):e0245387.
7 Abitbol CL, Rodriguez MM. The long-term renal and cardiovascular consequences of prematurity. *Nat Rev Nephrol*. 2012;8(5):265–274.
8 O'Reilly M, Sozo F, Harding R. Impact of preterm birth and bronchopulmonary dysplasia on the developing lung: long-term consequences for respiratory health. *Clin Exp Pharmacol Physiol*. 2013;40(11):765–773.
9 Goldenberg RL, Culhane JF, Iams JD, Romero R. Epidemiology and causes of preterm birth. *Lancet*. 2008;371(9606):75–84.
10 Romero R, Dey SK, Fisher SJ. Preterm labor: one syndrome, many causes. *Science*. 2014;345(6198):760–765.
11 Romero R, Espinoza J, Goncalves LF, Kusanovic JP, Friel LA, Nien JK. Inflammation in preterm and term labour and delivery. *Semin Fetal Neonatal Med*. 2006;11(5):317–326.
12 Gomez-Lopez N, Galaz J, Miller D, et al. The immunobiology of preterm labor and birth: intra-amniotic inflammation or breakdown of maternal-fetal homeostasis. *Reproduction*. 2022;164(2):R11–R45.
13 Yoon BH, Romero R, Moon JB, et al. Clinical significance of intra-amniotic inflammation in patients with preterm labor and intact membranes. *Am J Obstet Gynecol*. 2001;185(5):1130–1136.
14 Nien JK, Yoon BH, Espinoza J, et al. A rapid MMP-8 bedside test for the detection of intra-amniotic inflammation identifies patients at risk for imminent preterm delivery. *Am J Obstet Gynecol*. 2006;195(4):1025–1030.
15 Kim KW, Romero R, Park HS, et al. A rapid matrix metalloproteinase-8 bedside test for the detection of intraamniotic inflammation in women with preterm premature rupture of membranes. *Am J Obstet Gynecol*. 2007;197(3):292.e1–292.e5.
16 Cobo T, Aldecoa V, Holeckova M, et al. A rapid amniotic fluid interleukin-6 assessment for the identification of intra-amniotic inflammation in women with preterm labor and intact membranes. *Fetal Diagn Ther*. 2021;48(5):327–332.
17 Gibbs RS, Romero R, Hillier SL, Eschenbach DA, Sweet RL. A review of premature birth and subclinical infection. *Am J Obstet Gynecol*. 1992;166(5):1515–1528.
18 Romero R, Gomez R, Chaiworapongsa T, Conoscenti G, Kim JC, Kim YM. The role of infection in preterm labour and delivery. *Paediatr Perinat Epidemiol*. 2001;15(Suppl 2):41–56.
19 Goncalves LF, Chaiworapongsa T, Romero R. Intrauterine infection and prematurity. *Ment Retard Dev Disabil Res Rev*. 2002;8(1):3–13.
20 Romero R, Miranda J, Chaiworapongsa T, et al. Prevalence and clinical significance of sterile intra-amniotic inflammation in patients with preterm labor and intact membranes. *Am J Reprod Immunol*. 2014;72(5):458–474.
21 Romero R, Grivel JC, Tarca AL, et al. Evidence of perturbations of the cytokine network in preterm labor. *Am J Obstet Gynecol*. 2015;213(6):836.e1–836.e18.
22 Bhatti G, Romero R, Rice GE, et al. Compartmentalized profiling of amniotic fluid cytokines in women with preterm labor. *PLoS One*. 2020;15(1):e0227881.
23 Combs CA, Gravett M, Garite TJ, et al. Amniotic fluid infection, inflammation, and colonization in preterm labor with intact membranes. *Am J Obstet Gynecol*. 2014;210(2):125.e1–125.e15.
24 Romero R, Miranda J, Chaiworapongsa T, et al. A novel molecular microbiologic technique for the rapid diagnosis of microbial invasion of the amniotic cavity and intra-amniotic infection in preterm labor with intact membranes. *Am J Reprod Immunol*. 2014;71(4):330–358.
25 Romero R, Miranda J, Chaiworapongsa T, et al. Sterile intra-amniotic inflammation in asymptomatic patients with a sonographic short cervix: prevalence and clinical significance. *J Matern Fetal Neonatal Med*. 2015;28(11):1343–1359.
26 Romero R, Miranda J, Chaemsaithong P, et al. Sterile and microbial-associated intra-amniotic inflammation in preterm prelabor rupture of membranes. *J Matern Fetal Neonatal Med*. 2015;28(12):1394–1409.
27 Burnham P, Gomez-Lopez N, Heyang M, et al. Separating the signal from the noise in metagenomic cell-free DNA sequencing. *Microbiome*. 2020;8(1):18.
28 Romero R, Mazor M, Tartakovsky B. Systemic administration of interleukin-1 induces preterm parturition in mice. *Am J Obstet Gynecol*. 1991;165(4 Pt 1):969–971.
29 Romero R, Tartakovsky B. The natural interleukin-1 receptor antagonist prevents interleukin-1-induced preterm delivery in mice. *Am J Obstet Gynecol*. 1992;167(4 Pt 1):1041–1045.
30 Motomura K, Romero R, Garcia-Flores V, et al. The alarmin interleukin-1α causes preterm birth through the NLRP3 inflammasome. *Mol Hum Reprod*. 2020;26(9):712–726.
31 Robertson SA, Christiaens I, Dorian CL, et al. Interleukin-6 is an essential determinant of on-time parturition in the mouse. *Endocrinology*. 2010;151(8):3996–4006.
32 Gomez-Lopez N, Olson DM, Robertson SA. Interleukin-6 controls uterine Th9 cells and CD8(+) T regulatory cells to accelerate parturition in mice. *Immunol Cell Biol*. 2016;94(1):79–89.
33 Gotestam Skorpen C, Hoeltzenbein M, Tincani A, et al. The EULAR points to consider for use of antirheumatic drugs before pregnancy, and during pregnancy and lactation. *Ann Rheum Dis*. 2016;75(5):795–810.
34 Hoeltzenbein M, Beck E, Rajwanshi R, et al. Tocilizumab use in pregnancy: analysis of a global safety database including data from clinical trials and post-marketing data. *Semin Arthritis Rheum*. 2016;46(2):238–245.
35 Ghalandari N, Crijns H, Bergman JEH, Dolhain R, van Puijenbroek EP, Hazes JMW. Reported congenital malformations after exposure to non-tumour necrosis factor inhibitor biologics: a

retrospective comparative study in EudraVigilance. *Br J Clin Pharmacol*. 2022;88(12):5378–5388.
36 San-Juan R, Barbero P, Fernandez-Ruiz M, et al. Incidence and clinical profiles of COVID-19 pneumonia in pregnant women: a single-centre cohort study from Spain. *eClinicalMedicine*. 2020;23:100407.
37 Naqvi M, Zakowski P, Glucksman L, Smithson S, Burwick RM. Tocilizumab and remdesivir in a pregnant patient with coronavirus disease 2019 (COVID-19). *Obstet Gynecol*. 2020;136(5):1025–1029.
38 Recovery Collaborative Group. Tocilizumab in patients admitted to hospital with COVID-19 (RECOVERY): a randomised, controlled, open-label, platform trial. *Lancet*. 2021;397(10285):1637–1645.
39 Martinez-Sanchez N, De la Calle Fernandez-Miranda M, Bartha JL. Safety profile of treatments administered in COVID 19 infection in pregnant women. *Clin Invest Ginecol Obstet*. 2021;48(3):100663.
40 Jiménez-Lozano I, Caro-Teller JM, Fernández-Hidalgo N, et al. Safety of tocilizumab in COVID-19 pregnant women and their newborn: a retrospective study. *J Clin Pharm Ther*. 2021;46(4):1062–1070.
41 Jorgensen SC, Tabbara N, Burry L. A review of COVID-19 therapeutics in pregnancy and lactation. *Obstet Med*. 2022;15(4):225–232.
42 Wakabayashi A, Sawada K, Nakayama M, et al. Targeting interleukin-6 receptor inhibits preterm delivery induced by inflammation. *Mol Hum Reprod*. 2013;19(11):718–726.
43 Cappelletti M, Presicce P, Lawson MJ, et al. Type I interferons regulate susceptibility to inflammation-induced preterm birth. *JCI Insight*. 2017;2(5):e91288.
44 Fenwick N, Griffin G, Gauthier C. The welfare of animals used in science: how the "Three Rs" ethic guides improvements. *Can Vet J*. 2009;50(5):523–530.
45 Pique-Regi R, Romero R, Tarca AL, et al. Single cell transcriptional signatures of the human placenta in term and preterm parturition. *Elife*. 2019;8:e52004.
46 Bray NL, Pimentel H, Melsted P, Pachter L. Near-optimal probabilistic RNA-seq quantification. *Nat Biotechnol*. 2016;34(5):525–527.
47 Melsted P, Booeshaghi AS, Liu L, et al. Modular, efficient and constant-memory single-cell RNA-seq preprocessing. *Nat Biotechnol*. 2021;39(7):813–818.
48 Alvarez M, Rahmani E, Jew B, et al. Enhancing droplet-based single-nucleus RNA-seq resolution using the semi-supervised machine learning classifier DIEM. *Sci Rep*. 2020;10(1):11019.
49 Hafemeister C, Satija R. Normalization and variance stabilization of single-cell RNA-seq data using regularized negative binomial regression. *Genome Biol*. 2019;20(1):296.
50 Stuart T, Butler A, Hoffman P, et al. Comprehensive integration of single-cell data. *Cell*. 2019;177(7):1888–1902.e21.
51 Korsunsky I, Millard N, Fan J, et al. Fast, sensitive and accurate integration of single-cell data with Harmony. *Nat Methods*. 2019;16(12):1289–1296.
52 Garcia-Flores V, Romero R, Peyvandipour A, et al. A single-cell atlas of murine reproductive tissues during preterm labor. *Cell Rep*. 2023;42(1):111846.
53 Gomez-Lopez N, Romero R, Arenas-Hernandez M, et al. Intra-amniotic administration of lipopolysaccharide induces spontaneous preterm labor and birth in the absence of a body temperature change. *J Matern Fetal Neonatal Med*. 2018;31(4):439–446.
54 Garcia-Flores V, Romero R, Miller D, et al. Inflammation-induced adverse pregnancy and neonatal outcomes can Be improved by the immunomodulatory peptide exendin-4. *Front Immunol*. 2018;9:1291.
55 Faro J, Romero R, Schwenkel G, et al. Intra-amniotic inflammation induces preterm birth by activating the NLRP3 inflammasome. *Biol Reprod*. 2019;100(5):1290–1305.
56 Motomura K, Romero R, Galaz J, et al. Fetal and maternal NLRP3 signaling is required for preterm labor and birth. *JCI Insight*. 2022;7(16):e158238.
57 Galaz J, Romero R, Arenas-Hernandez M, Panaitescu B, Garcia-Flores V, Gomez-Lopez N. A protocol for evaluating vital signs and maternal-fetal parameters using high-resolution ultrasound in pregnant mice. *STAR Protoc*. 2020;1(3):100134.
58 Galaz J, Romero R, Arenas-Hernandez M, Panaitescu B, Para R, Gomez-Lopez N. Betamethasone as a potential treatment for preterm birth associated with sterile intra-amniotic inflammation: a murine study. *J Perinat Med*. 2021;49(7):897–906.
59 Galaz J, Romero R, Arenas-Hernandez M, et al. Clarithromycin prevents preterm birth and neonatal mortality by dampening alarmin-induced maternal-fetal inflammation in mice. *BMC Pregnancy Childbirth*. 2022;22(1):503.
60 Xu Y, Romero R, Miller D, et al. An M1-like macrophage polarization in decidual tissue during spontaneous preterm labor that is attenuated by rosiglitazone treatment. *J Immunol*. 2016;196(6):2476–2491.
61 Hill JM, Lim MA, Stone MM. In: Gozes I, ed. *Developmental milestones in the newborn mouse*. Totowa, NJ: Humana Press Inc; 2008.
62 Feather-Schussler DN, Ferguson TS. A battery of motor tests in a neonatal mouse model of cerebral palsy. *J Vis Exp*. 2016;117:53569.
63 Berkowitz BA, Romero R, Podolsky RH, et al. QUEST MRI assessment of fetal brain oxidative stress in utero. *Neuroimage*. 2019;200:601–606.
64 Berkowitz BA, Bredell BX, Davis C, Samardzija M, Grimm C, Roberts R. Measuring in vivo free radical production by the outer retina. *Invest Ophthalmol Vis Sci*. 2015;56(13):7931–7938.
65 Berkowitz BA. Adult and newborn rat inner retinal oxygenation during carbogen and 100% oxygen breathing. Comparison using magnetic resonance imaging delta Po2 mapping. *Invest Ophthalmol Vis Sci*. 1996;37(10):2089–2098.
66 Kadam L, Gomez-Lopez N, Mial TN, Kohan-Ghadr HR, Drewlo S. Rosiglitazone regulates TLR4 and rescues HO-1 and NRF2 expression in myometrial and decidual macrophages in inflammation-induced preterm birth. *Reprod Sci*. 2017;24(12):1590–1599.
67 Arenas-Hernandez M, Romero R, Xu Y, et al. Effector and activated T cells induce preterm labor and birth that is prevented by treatment with progesterone. *J Immunol*. 2019;202(9):2585–2608.
68 Bushnell B. BBMap: a fast, accurate, splice-aware aligner. In: *Conference: 9th annual Genomics of energy & Environment Meeting*. Walnut Creek, CA, USA: United States; 2014 [cited 2023 Oct 9]. Available from: https://www.osti.gov/servlets/purl/1241166.
69 Wood DE, Lu J, Langmead B. Improved metagenomic analysis with Kraken 2. *Genome Biol*. 2019;20(1):257.
70 Lu J, Breitwieser FP, Thielen P, Salzberg SL. Bracken: estimating species abundance in metagenomics data. *PeerJ Comput Sci*. 2017;3:e104.
71 McMurdie PJ, Holmes S. phyloseq: an R package for reproducible interactive analysis and graphics of microbiome census data. *PLoS One*. 2013;8(4):e61217.
72 Romero R, Mazor M, Munoz H, Gomez R, Galasso M, Sherer DM. The preterm labor syndrome. *Ann N Y Acad Sci*. 1994;734:414–429.
73 Norwitz ER, Robinson JN, Challis JR. The control of labor. *N Engl J Med*. 1999;341(9):660–666.
74 Romero R, Espinoza J, Kusanovic JP, et al. The preterm parturition syndrome. *BJOG*. 2006;113 Suppl 3(Suppl 3):17–42.
75 Smith R. Parturition. *N Engl J Med*. 2007;356(3):271–283.
76 Galaz J, Motomura K, Romero R, et al. A key role for NLRP3 signaling in preterm labor and birth driven by the alarmin S100B. *Transl Res*. 2023;259:46–61.
77 Williams MC, O'Brien WF, Nelson RN, Spellacy WN. Histologic chorioamnionitis is associated with fetal growth restriction in term and preterm infants. *Am J Obstet Gynecol*. 2000;183(5):1094–1099.
78 Levy M, Kovo M, Feldstein O, et al. The effect of concomitant histologic chorioamnionitis in pregnancies complicated by fetal growth restriction. *Placenta*. 2021;104:51–56.
79 Chalupska M, Kacerovsky M, Stranik J, et al. Intra-amniotic infection and sterile intra-amniotic inflammation in cervical insufficiency with prolapsed fetal membranes: clinical implications. *Fetal Diagn Ther*. 2021;48(1):58–69.
80 Matulova J, Kacerovsky M, Bolehovska R, et al. Intra-amniotic inflammation and birth weight in pregnancies with preterm labor with intact membranes: a retrospective cohort study. *Front Pediatr*. 2022;10:916780.
81 Heyser CJ. Assessment of developmental milestones in rodents. *Curr Protoc Neurosci*. 2004 Chapter 8:Unit 8.18.
82 Colin AA, McEvoy C, Castile RG. Respiratory morbidity and lung function in preterm infants of 32 to 36 weeks' gestational age. *Pediatrics*. 2010;126(1):115–128.
83 Stoll BJ, Hansen NI, Bell EF, et al. Neonatal outcomes of extremely preterm infants from the NICHD Neonatal Research Network. *Pediatrics*. 2010;126(3):443–456.
84 Viscardi RM. Perinatal inflammation and lung injury. *Semin Fetal Neonatal Med*. 2012;17(1):30–35.
85 Jobe AH. Effects of chorioamnionitis on the fetal lung. *Clin Perinatol*. 2012;39(3):441–457.
86 Villamor-Martinez E, Alvarez-Fuente M, Ghazi AMT, et al. Association of chorioamnionitis with bronchopulmonary dysplasia among preterm infants: a systematic review, meta-analysis, and metaregression. *JAMA Netw Open*. 2019;2(11):e1914611.

87 La Rosa PS, Warner BB, Zhou Y, et al. Patterned progression of bacterial populations in the premature infant gut. *Proc Natl Acad Sci U S A*. 2014;111(34):12522–12527.
88 Underwood MA, Sohn K. The microbiota of the extremely preterm infant. *Clin Perinatol*. 2017;44(2):407–427.
89 Lim AI, McFadden T, Link VM, et al. Prenatal maternal infection promotes tissue-specific immunity and inflammation in offspring. *Science*. 2021;373(6558):eabf3002.
90 Neu J, Walker WA. Necrotizing enterocolitis. *N Engl J Med*. 2011;364(3):255–264.
91 Been JV, Lievense S, Zimmermann LJ, Kramer BW, Wolfs TG. Chorioamnionitis as a risk factor for necrotizing enterocolitis: a systematic review and meta-analysis. *J Pediatr*. 2013;162(2):236–242.e2.
92 Fullerton JN. Use of non-steroidal anti-inflammatory drugs (NSAIDs) as immunomodulatory agents. *BMJ*. 2013;347:f4984.
93 Pacher P, Nivorozhkin A, Szabo C. Therapeutic effects of xanthine oxidase inhibitors: renaissance half a century after the discovery of allopurinol. *Pharmacol Rev*. 2006;58(1):87–114.
94 Khanna D, Fitzgerald JD, Khanna PP, et al. 2012 American College of Rheumatology guidelines for management of gout. Part 1: systematic nonpharmacologic and pharmacologic therapeutic approaches to hyperuricemia. *Arthritis Care Res (Hoboken)*. 2012;64(10):1431–1446.
95 Antonucci R, Zaffanello M, Puxeddu E, et al. Use of non-steroidal anti-inflammatory drugs in pregnancy: impact on the fetus and newborn. *Curr Drug Metab*. 2012;13(4):474–490.
96 Birru Talabi M, Clowse MEB. Antirheumatic medications in pregnancy and breastfeeding. *Curr Opin Rheumatol*. 2020;32(3):238–246.
97 American College of Obstetricians and Gynecologists. Committee opinion no. 713: antenatal corticosteroid therapy for fetal maturation. *Obstet Gynecol*. 2017;130(2):e102–e109.
98 McGoldrick E, Stewart F, Parker R, Dalziel SR. Antenatal corticosteroids for accelerating fetal lung maturation for women at risk of preterm birth. *Cochrane Database Syst Rev*. 2020;12(12):CD004454.
99 Lee J, Romero R, Kim SM, Chaemsaithong P, Yoon BH. A new antibiotic regimen treats and prevents intra-amniotic inflammation/infection in patients with preterm PROM. *J Matern Fetal Neonatal Med*. 2016;29(17):2727–2737.
100 Oh KJ, Romero R, Park JY, et al. Evidence that antibiotic administration is effective in the treatment of a subset of patients with intra-amniotic infection/inflammation presenting with cervical insufficiency. *Am J Obstet Gynecol*. 2019;221(2):140.e1–140.e18.
101 Yoon BH, Romero R, Park JY, et al. Antibiotic administration can eradicate intra-amniotic infection or intra-amniotic inflammation in a subset of patients with preterm labor and intact membranes. *Am J Obstet Gynecol*. 2019;221(2):142.e1–142.e22.
102 Kacerovsky M, Romero R, Stepan M, et al. Antibiotic administration reduces the rate of intraamniotic inflammation in preterm prelabor rupture of the membranes. *Am J Obstet Gynecol*. 2020;223(1):114.e1–114.e20.
103 Pereira A, Cruz-Melguizo S, Adrien M, Fuentes L, Marin E, Perez-Medina T. Clinical course of coronavirus disease-2019 in pregnancy. *Acta Obstet Gynecol Scand*. 2020;99(7):839–847.
104 Abdullah S, Bashir N, Mahmood N. Use of intravenous tocilizumab in pregnancy for severe coronavirus disease 2019 pneumonia: two case reports. *J Med Case Rep*. 2021;15(1):426.
105 Jorgensen SCJ, Lapinsky SE. Tocilizumab for coronavirus disease 2019 in pregnancy and lactation: a narrative review. *Clin Microbiol Infect*. 2022;28(1):51–57.
106 Péju E, Belicard F, Silva S, et al. Management and outcomes of pregnant women admitted to intensive care unit for severe pneumonia related to SARS-CoV-2 infection: the multicenter and international COVIDPREG study. *Intensive Care Med*. 2022;48(9):1185–1196.
107 Ray A, Samra T, Mahajan V, et al. Characteristics and outcomes of parturients with COVID-19, admitted to a critical care unit: a single-center retrospective observational study. *J Family Med Prim Care*. 2022;11(10):6478–6486.
108 Isaac B, Hazari K, Harb DK, et al. Maternal and fetal outcome in pregnant women with critical COVID-19 treated with tocilizumab in a tertiary care hospital in dubai. *Cureus*. 2023;15(1):e34395.
109 Nakajima K, Watanabe O, Mochizuki M, Nakasone A, Ishizuka N, Murashima A. Pregnancy outcomes after exposure to tocilizumab: a retrospective analysis of 61 patients in Japan. *Mod Rheumatol*. 2016;26(5):667–671.
110 Saito J, Yakuwa N, Takai C, et al. Tocilizumab concentrations in maternal serum and breast milk during breastfeeding and a safety assessment in infants: a case study. *Rheumatology (Oxford)*. 2018;57(8):1499–1501.
111 Raia-Barjat T, Digonnet M, Giraud A, et al. Animal models of chorioamnionitis: considerations for translational medicine. *Biomedicines*. 2022;10(4):811.
112 Barton JR, Sibai BM. Severe sepsis and septic shock in pregnancy. *Obstet Gynecol*. 2012;120(3):689–706.
113 Escobar MF, Echavarría MP, Zambrano MA, Ramos I, Kusanovic JP. Maternal sepsis. *Am J Obstet Gynecol MFM*. 2020;2(3):100149.
114 Conde-Agudelo A, Romero R, Jung EJ, Garcia Sánchez Á J. Management of clinical chorioamnionitis: an evidence-based approach. *Am J Obstet Gynecol*. 2020;223(6):848–869.
115 Yoshimura K, Hirsch E. Interleukin-6 is neither necessary nor sufficient for preterm labor in a murine infection model. *J Soc Gynecol Investig*. 2003;10(7):423–427.
116 Prins JR, Gomez-Lopez N, Robertson SA. Interleukin-6 in pregnancy and gestational disorders. *J Reprod Immunol*. 2012;95(1-2):1–14.
117 Bredeson S, Papaconstantinou J, Deford JH, et al. HMGB1 promotes a p38MAPK associated non-infectious inflammatory response pathway in human fetal membranes. *PLoS One*. 2014;9(12):e113799.
118 Menon R, Behnia F, Polettini J, Saade GR, Campisi J, Velarde M. Placental membrane aging and HMGB1 signaling associated with human parturition. *Aging (Albany NY)*. 2016;8(2):216–230.
119 Plazyo O, Romero R, Unkel R, et al. HMGB1 induces an inflammatory response in the chorioamniotic membranes that is partially mediated by the inflammasome. *Biol Reprod*. 2016;95(6):130.
120 Gomez-Lopez N, Romero R, Panaitescu B, et al. Inflammasome activation during spontaneous preterm labor with intra-amniotic infection or sterile intra-amniotic inflammation. *Am J Reprod Immunol*. 2018;80(5):e13049.
121 Gomez-Lopez N, Romero R, Tarca AL, et al. Gasdermin D: evidence of pyroptosis in spontaneous preterm labor with sterile intra-amniotic inflammation or intra-amniotic infection. *Am J Reprod Immunol*. 2019;82(6):e13184.
122 Motomura K, Romero R, Galaz J, et al. RNA sequencing reveals distinct immune responses in the chorioamniotic membranes of women with preterm labor and microbial or sterile intra-amniotic inflammation. *Infect Immun*. 2021;89(5):e00819–e00820.
123 Motomura K, Romero R, Plazyo O, et al. The alarmin S100A12 causes sterile inflammation of the human chorioamniotic membranes as well as preterm birth and neonatal mortality in mice†. *Biol Reprod*. 2021;105(6):1494–1509.
124 Gomez-Lopez N, Romero R, Garcia-Flores V, et al. Inhibition of the NLRP3 inflammasome can prevent sterile intra-amniotic inflammation, preterm labor/birth, and adverse neonatal outcomes†. *Biol Reprod*. 2019;100(5):1306–1318.
125 Mano Y, Shibata K, Sumigama S, et al. Tocilizumab inhibits interleukin-6-mediated matrix metalloproteinase-2 and -9 secretions from human amnion cells in preterm premature rupture of membranes. *Gynecol Obstet Invest*. 2009;68(3):145–153.
126 Barrichon M, Hadi T, Wendremaire M, et al. Dose-dependent biphasic leptin-induced proliferation is caused by non-specific IL-6/NF-kappaB pathway activation in human myometrial cells. *Br J Pharmacol*. 2015;172(12):2974–2990.
127 Pennington KA, Oestreich AK, Cataldo KH, et al. Conditional knockout of leptin receptor in the female reproductive tract reduces fertility due to parturition defects in mice. *Biol Reprod*. 2022;107(2):546–556.
128 Branham KKR, Sherman E, Golzy M, Drobnis EZ, Schulz LC. Association of serum leptin at 24-28 weeks gestation with initiation and progression of labor in women. *Sci Rep*. 2022;12(1):16016.
129 Tada Y, Sakai M, Nakao Y, Maruyama A, Ono N, Koarada S. Placental transfer of tocilizumab in a patient with rheumatoid arthritis. *Rheumatology (Oxford)*. 2019;58(9):1694–1695.
130 Galinsky R, Polglase GR, Hooper SB, Black MJ, Moss TJ. The consequences of chorioamnionitis: preterm birth and effects on development. *J Pregnancy*. 2013;2013:412831.
131 Jin C, Londono I, Mallard C, Lodygensky GA. New means to assess neonatal inflammatory brain injury. *J Neuroinflammation*. 2015;12:180.
132 Han VX, Patel S, Jones HF, et al. Maternal acute and chronic inflammation in pregnancy is associated with common neurodevelopmental disorders: a systematic review. *Transl Psychiatry*. 2021;11(1):71.

133 Han VX, Patel S, Jones HF, Dale RC. Maternal immune activation and neuroinflammation in human neurodevelopmental disorders. *Nat Rev Neurol*. 2021;17(9):564–579.
134 Yoon BH, Jun JK, Romero R, et al. Amniotic fluid inflammatory cytokines (interleukin-6, interleukin-1beta, and tumor necrosis factor-alpha), neonatal brain white matter lesions, and cerebral palsy. *Am J Obstet Gynecol*. 1997;177(1):19–26.
135 Al-Haddad BJS, Jacobsson B, Chabra S, et al. Long-term risk of neuropsychiatric disease after exposure to infection in utero. *JAMA Psychiatr*. 2019;76(6):594–602.
136 Leviton A. Preterm birth and cerebral palsy: is tumor necrosis factor the missing link? *Dev Med Child Neurol*. 1993;35(6):553–558.
137 Yoon BH, Romero R, Jun JK, et al. Amniotic fluid cytokines (interleukin-6, tumor necrosis factor-alpha, interleukin-1 beta, and interleukin-8) and the risk for the development of bronchopulmonary dysplasia. *Am J Obstet Gynecol*. 1997;177(4):825–830.
138 Wolfs TG, Kallapur SG, Polglase GR, et al. IL-1alpha mediated chorioamnionitis induces depletion of FoxP3+ cells and ileal inflammation in the ovine fetal gut. *PLoS One*. 2011;6(3):e18355.
139 Wolfs TG, Kramer BW, Thuijls G, et al. Chorioamnionitis-induced fetal gut injury is mediated by direct gut exposure of inflammatory mediators or by lung inflammation. *Am J Physiol Gastrointest Liver Physiol*. 2014;306(5):G382–G393.
140 Nikiforou M, Kemp MW, van Gorp RH, et al. Selective IL-1alpha exposure to the fetal gut, lung, and chorioamnion/skin causes intestinal inflammatory and developmental changes in fetal sheep. *Lab Invest*. 2016;96(1):69–80.
141 Nguyen DN, Thymann T, Goericke-Pesch SK, et al. Prenatal intra-amniotic endotoxin induces fetal gut and lung immune responses and postnatal systemic inflammation in preterm pigs. *Am J Pathol*. 2018;188(11):2629–2643.
142 Elgin TG, Fricke EM, Gong H, et al. Fetal exposure to maternal inflammation interrupts murine intestinal development and increases susceptibility to neonatal intestinal injury. *Dis Model Mech*. 2019;12(10):dmm040808.
143 Cuna A, Morowitz MJ, Ahmed I, Umar S, Sampath V. Dynamics of the preterm gut microbiome in health and disease. *Am J Physiol Gastrointest Liver Physiol*. 2021;320(4):G411–G419.
144 Tamburini S, Shen N, Wu HC, Clemente JC. The microbiome in early life: implications for health outcomes. *Nat Med*. 2016;22(7):713–722.
145 Schreurs R, Baumdick ME, Sagebiel AF, et al. Human fetal TNF-α-cytokine-producing CD4(+) effector memory T cells promote intestinal development and mediate inflammation early in life. *Immunity*. 2019;50(2):462–476.e8.
146 Li N, van Unen V, Abdelaal T, et al. Memory CD4(+) T cells are generated in the human fetal intestine. *Nat Immunol*. 2019;20(3):301–312.
147 Halkias J, Rackaityte E, Hillman SL, et al. CD161 contributes to prenatal immune suppression of IFNgamma-producing PLZF+ T cells. *J Clin Invest*. 2019;129(9):3562–3577.
148 Puri K, Taft DH, Ambalavanan N, Schibler KR, Morrow AL, Kallapur SG. Association of chorioamnionitis with aberrant neonatal gut colonization and adverse clinical outcomes. *PLoS One*. 2016;11(9):e0162734.
149 Ma X, Xu T, Qian M, Zhang Y, Yang Z, Han X. Faecal microbiota transplantation alleviates early-life antibiotic-induced gut microbiota dysbiosis and mucosa injuries in a neonatal piglet model. *Microbiol Res*. 2021;255:126942.
150 Bhatia R, Sharma S, Bhadada SK, Bishnoi M, Kondepudi KK. Lactic acid bacterial supplementation ameliorated the lipopolysaccharide-induced gut inflammation and dysbiosis in mice. *Front Microbiol*. 2022;13:930928.